2016

Numerical Simulation of High Velocity Impact of a Single Polymer Particle during Cold Spray Deposition

Sagar P. Shah
University of Massachusetts Amherst

NUMERICAL SIMULATION OF HIGH VELOCITY IMPACT OF A SINGLE POLYMER PARTICLE DURING COLD SPRAY

A Thesis Presented

by

SAGAR PANKAJ SHAH

Submitted to the Graduate School of the
University of Massachusetts Amherst in partial fulfillment
of the requirements for the degree of

MASTER OF SCIENCE IN MECHANICAL ENGINEERING

September 2016

Mechanical and Industrial Engineering

NUMERICAL SIMULATION OF HIGH VELOCITY IMPACT OF A SINGLE POLYMER PARTICLE DURING COLD SPRAY DEPOSITION

A Thesis Presented

by

SAGAR PANKAJ SHAH

_____

Jonghyun Lee, Co-Chair

_____

Jonathan P. Rothstein, Co-Chair

_____

David P. Schmidt, Member

_____

Sundar Krishnamurty, Department Head

Department of Mechanical and Industrial Engineering

ACKNOWLEDGEMENTS

First and foremost, I wish to express my sincere gratitude and respect to my co-advisor Professor Jonghyun Lee. His invaluable help and continuous support guided me throughout every stage of my research.

I would like to thank my co-advisor Professor Jonathan Rothstien for his extensive technical contributions and insightful discussions, which have helped improve this research greatly.

I thank Professor David Schmidt for leading the Cold Spray Project at University of Massachusetts, Amherst and the Army Research Laboratory for their financial support that made this research possible.

I dedicate this dissertation to my friends and family for their endless love, support and encouragement throughout my life.

ABSTRACT

NUMERICAL SIMULATION OF HIGH VELOCITY IMPACT OF A SINGLE POLYMER PARTICLE DURING COLD SPRAY

SEPTEMBER 2016

SAGAR PANKAJ SHAH, B.E., K.J. SOMAIYA COLLEGE OF ENGINEERING

M.S., UNIVERSITY OF MASSACHUSETTS AMHERST

Directed by: Professor Jonghyun Lee

The cold spray process is an additive manufacturing technology primarily suited for ductile metals, and mainly utilized in coating surfaces, manufacturing of freeform parts and repair of damaged components. The process involves acceleration of solid micro-particles in a supersonic gas flow and coating build-up by bonding upon high velocity impact onto a substrate. Coating deposition relies on the kinetic energy of the particles. The main objective of this study was to investigate the mechanics of polymer cold spray process and deformation behavior of polymers to improve technological implementation of the process.

A finite element model was created to simulate metal particle impact for copper and aluminum. These results were compared to the numerical and experimental results found in the literature to validate the model. This model was then extended to cover a wide range of impact conditions, in order to reveal the governing mechanisms of particle impact and rebound during cold spray.

A systematic analysis of a single high-density polyethylene particle impacting on a semi-infinite high density polyethylene substrate was carried out for initial velocities ranging between 150m/s and 250m/s by using the finite element analysis software ABAQUS. A series of numerical simulations were performed to study the effect of a number of key parameters on the particle impact dynamics. These key parameters include: particle impact velocity, particle temperature, particle diameter, and particle density, composition of the polyethylene particle, surface composition and the thickness of a polyethylene film on a hard metal substrate. The effect of these parameter variations were quantified by tracking the particle temperature, deformation, plastic strain and rebound kinetic energy. The variation of these parameters helped define a window of deposition where the particle is mostly likely to adhere to the substrate.

TABLE OF CONTENTS

Page

LIST OF TABLES

Table Page

LIST OF FIGURES

Figure Page

CHAPTER 1

INTRODUCTION TO COLD SPRAY

Cold Spraying or Gas Dynamic Cold Spraying (GDCS) is a coating technique that uses high speed particle impact over a substrate for deposition. This technique is useful for creating either metallic or polymeric coatings. Cold Spraying is very effective for corrosion resistant coatings, wear resistant coatings, dimensional restoration and repairs, anti-microbial surface depositions [1]. Consequently, it has gained attention in aerospace, automobile manufacturing and chemical industries.

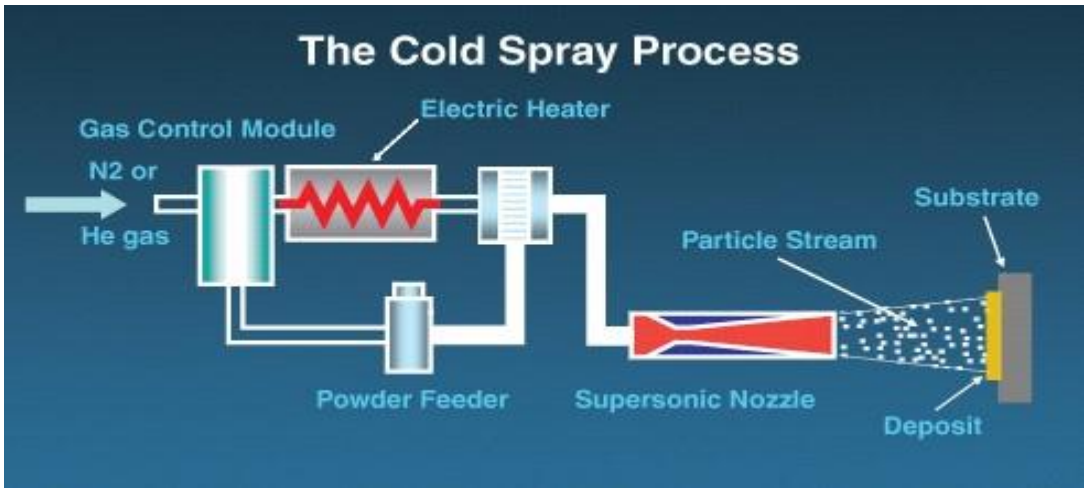

Figure 1-1: The Cold Spray Process Setup.

In this process, the particles with size ranging from 5-70 μm in diameter are accelerated at high velocities, as high as MACH 3, by a high speed gas flow through a convergent-divergent de Laval nozzle. The impact of particle at such high velocities forms a coating due to extensive plastic deformation. The entire process occurs at temperatures below the melting point of the particle and the process is named cold spraying in contrast to conventional thermal spraying which takes advantage of melting of materials.

Although this process is being implemented extensively in many industries, the actual bonding mechanism is still unclear. One of the most recent and prevailing hypotheses describes the bonding is resulted from excessive plastic deformations [2]. The deformation disrupts the oxide film formed on the substrate and particle surface providing conformal contact owing to high local pressure leading to bonding [2]. The jetting disrupts the oxide film forming potential deposition sites on the substrate [3]. This hypothesis complies with the fact that a wide range of ductile materials have been deposited using cold spraying. If brittle materials (ceramics) are to be deposited, they need to be co-sprayed with ductile materials (metals or alloys) to ensure deposition [3]. It has been observed that deposition takes place at or beyond a certain velocity only called the critical velocity. The critical velocity depends on particle size, temperature and oxidation state of the particle and the substrate material [3]. This explains the need to define critical velocity to ensure high deposition efficiency.

Another theory that describes the bonding mechanism is the adiabatic shear instability which occurs at the particle substrate interface at or beyond critical velocity [4-6]. There has been extensive numerical and experimental research on the bonding mechanisms and deformation behavior. A number of different bonding mechanisms on the particle/substrate contact interface, induced by adiabatic shear instability have been proposed [4, 6-12]. When a particle travelling at or beyond the critical velocity, impacts on a substrate, a strong pressure field propagates spherically into the particle and substrate from the point of contact. As a result of the pressure gradient at the gap between the colliding surfaces, a shear load is generated and it accelerates the material laterally and causes localized shear straining. When the impact pressure and the respective deformations

are high enough, this shear straining leads to adiabatic shear instability where thermal softening is locally dominant over work strain and strain rate hardening, leading to a discontinuous jump in strain and temperature along with breakdown of flow stresses. This adiabatic shear instability phenomenon results in viscous flow of material in an outward flowing direction with temperatures close to melting temperature of the material [4-6].

1.1 Types of Cold Spray Process

Cold spraying processes can be described as high pressure and low pressure systems [13].

1.1.1 High Pressure System: Figure 1-2 shows a high pressure cold spraying configuration in which a gas stream and powder feeder stream are introduced into the inlet chamber of the nozzle. These systems utilize high pressure gases and have a dedicated compressor thus, often used in stationary cold spraying. As a result, the powder feeder should be capable of handling high gas pressure. Typically, helium and nitrogen gases are used at pressures above 1.5 MPa. These systems are generally used for spraying pure metal powders.

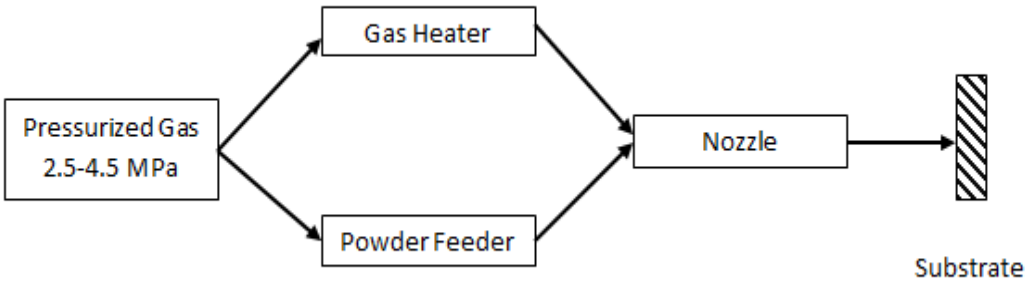

Figure 1-2: High Pressure Cold Spray system.

1.1.2 Low Pressure System: Figure 1-3 shows a system in which the powder stream is injected into the nozzle at a point where the gas has expanded to low pressure. Air at atmospheric pressure, drawn by the lower pressure nozzle injection point, is used for powder transport from the feeder. Since this system does not require a pressurized feeder, it is often used in portable cold spray systems and for spraying a mechanical mixture of metals and ceramic powders. The shocks due to the hammer effect of the impinging hard particles deform the deposited ductile particle thus requiring less input energy in the form of kinetic energy. Thus inclusion of ceramic components in the mixture provides high quality coatings with relatively low energy consumption.

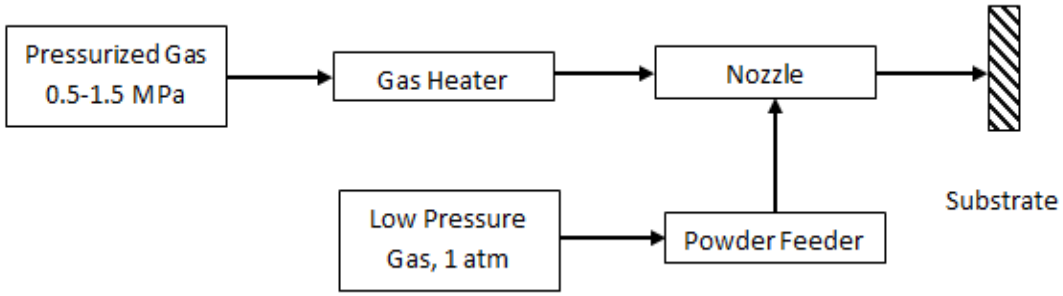

Figure 1-3: Low Pressure Cold Spray system.

1.2 Benefits of Cold Spray Process over conventional Thermal Spray Process

As compared to the conventional thermal spraying processes, cold spraying technique has the following advantages [14]:

a. Operating temperatures are lower, no bulk melting is required thus no combustion fuels or gases are required.

b. Easier to control phase transformation, retains composition/phases of initial particles.

c. Much less oxidation and low defect coatings, improving conductivity and corrosion resistance.

d. Eliminates solidification stresses, enables thicker coatings.

e. Lower heat input, thus reduces cooling requirements.

1.3 Uniqueness of this research

Cold spraying process shows excellent results when used for depositing ductile materials like copper and aluminum. Due to easily available properties for these materials, extensive research has been done involving copper and aluminum. These materials find many applications in aircraft, spacecraft, medical industry, automobiles etc. Recently, researchers have started focusing on Ti-6Al-4V alloy which is also an excellent material for cold spraying application due to its distinctive properties. It is light in weight, highly corrosion resistant and can withstand high temperatures. Despite all these merits, it is difficult to use Ti-6Al-4V for cold spraying due to its high cost, strength and toughness as compared to copper of aluminum.

Polymers have a wide range of applications that far exceeds that of any other materials available. Polymers can pose as good substitutes for metal coatings because of their corrosion resistance, high coating strength and cheap availability. Despite these advantages, it is difficult working with polymers because the impact of polymer powder differs significantly from metals. There are no rules of thumb available for defining the initial conditions for polymer particle impact. The critical velocities and the temperatures to achieve adhesion are unknown.

Another reason this research has not been pursued diligently is the complex response of a polymers when subjected to high strain rates. The process takes place at high speeds, deforming the material under very high strain rates, resulting in larger variations in

the behavior of the polymer with temperature and strain rate, making it even more difficult to obtain appropriate material data for any polymer at these conditions. Also, the built in material models in the finite element analysis software ABAQUS are not capable of completely outlining the material behavior and interpreting the temperature and strain rate dependent data. The material models available in ABAQUS fail to account for time dependent relaxation and creep and other phenomenon such as melting of material, chain interaction and bond entanglement. The concept of using polymers for cold spraying is still new and not much research has been done on it making this study so unique.

1.4 Aim and Objectives

The main purpose of this study is to simulate and investigate polymer impact. Originally, due to lack of appropriate data and the knowledge of material models for polymeric materials the study was conducted with copper as the base material. The copper model was used to compare the simulation results to those obtained from Yildirim *et al.* [15] and Li *et al.* [2] The impact of copper particle on aluminum substrate results were used to validate the model against experimental results [16]. The results obtained from the metal simulations were used to model polymer particle impact model.

1.5 Specific Objectives

a. The main purpose of this study is to develop a three dimensional model to predict the impact of a polymer particle onto a substrate.
b. To perform a detailed parametric study to investigate the effect of various physical parameters on the impact dynamics.
c. To develop a three dimensional model to effectively simulate the particle impact over an already deposited layer of polymer.

1.6 Arrangement of Thesis

The material presented is divided into 7 chapters. The present chapter (Chapter 1) provides an introduction to the cold spraying process, its types and its advantages over conventional spray techniques; this chapter also summarizes the research motivation and objectives.

In the first part of Chapter 2, a critical assessment of the relevant literature on metal cold spraying process is provided. The general features of cold spray process, a review of the previous numerical analyses related to the deformation characteristics of impacting particles and possible bonding mechanism suggested in literature are discussed. The second part systematically details the entire numerical method and the approach adapted based on the literature review; the results obtained are then validated against previous numerical and experimental work.

In Chapter 3, the model discussed in the previous chapter is extended to simulate particle impact for polymers. Again, the first part presents an in-depth review of how polymeric materials behave under different loading condition and discuss the material models or numerical methods developed to predict the polymeric material behavior. The latter half of this chapter shows the changes made to the metal cold spray model and the material model used for simulating the cold spray of polymers.

A series of numerical simulations were performed to study the effect of a number of key parameters on the particle impact dynamics in Chapter 4. These key parameters are discussed in this chapter; their effect are quantified and discussed.

In Chapter 5, key findings from the current research are summarized.

Future research plans, that will help improve the understanding of the mechanics of cold spray of polymers by building upon the findings of current research, are discussed in Chapter 6.

The references are mentioned at the end of the document.

CHAPTER 2

MODELING AND VALIDATION OF METAL PARTICLE IMPACT

2.1 Introduction

As discussed in the previous chapter, there are certain phenomena that are difficult to investigate experimentally during the cold spraying of particles. Thus, there is a need to investigate the process by numerical (finite element) simulations. The finite element analysis software ABAQUS is employed. Most of the particle impact simulations are carried out using copper as the particle and substrate material owing to the ductile nature of copper. The general features of cold spray process, a review of the previous numerical analyses related to impact dynamics and metal cold spraying literatures are discussed in the first part of this chapter. Based on the literature review, the numerical approach adopted is discussed next, followed by the results and discussions.

2.2 Literature Review

The effect of incorporating material damage was investigated by Gao [3]. The results showed that simulations with material damage cope well with excessive element distortion and the resultant output is more reasonable than that obtained without material damage. In addition, the meshing size has less effect on the output with the material damage than without material damage. Although, particle size has little effect on the morphologies of the deformed particles, it has some effect on the failure of elements at contact interfaces. The critical velocity for particle deposition could be estimated given the appropriate material properties. The coefficient of friction also has a little effect on the plastic

deformation and the temperature rise when changed from 0 to 0.5 using material damage [3].

Zhang [17] considered the effect of initial temperature of the particle and substrate, and the particle velocity on the deposition coating. The results showed that as the in-flight particle temperature was increased, the coating became denser and micro hardness and bond strength increased. Effective bonding between the particle and the substrate is most likely to happen when the adiabatic shear instability occurs at the contact interface and an interface jet forms [4, 9, 10]. Therefore, particle velocity and preheating temperature are the key factors in the formation of a coating. When the particle velocity and preheating temperature are too low, the particle will fracture upon impact, so no adiabatic shear instability occurs and it results in poor deposition. On the other hand, if the particle velocity and preheating temperature are too high, the particle will deform excessively or erode the substrate and other deposited particles. If the substrate is less prone to plastic deformation, the particle might even splash during the impact, which also makes it difficult to obtain effective deposition.

Later, Zhang established that the initial kinetic energy of the particle was the dominant factor in deposition behavior. Therefore, the effect of the initial temperature was not considered, and the substrate and particle temperatures were set to T_i = 298K [17].
The reported numerical results in literature have indicated that the flattening ratio of particles increase with the increase in particle impact velocity, which is comparable to the experimental results. Moreover, the temperature at localized contact interfaces rises remarkably due to the possible adiabatic shearing. Through numerical simulations in ABAQUS, Assadi *et al.* [4, 6, 10] found that the instability of adiabatic shear flow occurs

as particle velocity increases higher than a critical velocity. Therefore, they took this velocity as the actual critical velocity for particle deposition in cold spray. However, owing to the excessive distortion of elements at the local contact zones in simulation by the Lagrangian algorithm, this calculated critical velocity is much dependent on the meshing size [7, 18]. When Zhou *et al.* [12] used the Arbitrary Lagrangian Eulerian (ALE) method available in LS-DYNA to avoid the problems associated with the severe mesh distortion, no steep change of plastic strain or temperature was observed, which was used to indicate the onset of the shear instability by Assadi *et al.* [4, 6, 10]. Accordingly, it seemed that the steep change in plastic strain obtained by the Lagrangian method was attributed to the abnormal deformation of elements and could not be directly associated with the actual shear instability upon particle impacting.

The most important aspect of cold spraying simulation with Lagrangian algorithm is possible excessive distortion of elements near the contact surfaces at high velocities. The solution to this in ABAQUS is the use of Arbitrary Lagrangian Eulerian (ALE) adaptive mesh controls, element distortion control and material damage. As reported by Assadi *et al.* [4], although ALE adaptive mesh control can cope with excessive element distortion at high impact velocities, frequent remeshing results in non-conserving energy variation of the output set, and unrealistic shape of the out-flowing jet at the interface. Likewise, distortion control with length ratio in the higher range (0.5 to 1) can give unreasonable shape of the deformed particle as also obtained using ALE adaptive meshing. Thus, similar to ALE mesh control, distortion control is not quite suitable for modelling cold spraying impact simulations [3].

In addition, Schmidt *et al.* [6] also found the dependence of critical velocity on particle size by simulations using ABAQUS with the Lagrangian algorithm. It was established that for smaller dimensions, the occurrence of shear instabilities could be hindered by high cooling rates, higher strain rate and thus more profound strain rate hardening. Moreover, smaller particles experienced higher quench rates during powder production and showed intrinsically higher strength because of their finer microstructure. Thus smaller particles need higher critical velocity to initiate bonding. Although the experiments have shown the effect of particle size on critical velocity [8], their simulation results are believed to be unreasonable because recent studies have shown the effect of particle oxide films on critical velocity [7, 11, 19] which Schmidt *et al.* failed to consider. According to the fact that the powders of small sizes normally have higher oxygen concentrations than those of large sizes [11], it is expected that the oxide films on particle surfaces are the main factor influencing critical velocity besides the mechanical properties. However, these views need further experimental validation.

2.3 Numerical Method

As explained earlier, the time scale for investigating the impact of a particle is very small, of the order of 50-100ns, owing to high velocities. Thus, there is a need to simulate particle impact and study the impact dynamics by tracking the strains and the temperature induced. The model only predicts the deformation behavior during the impact, it does not capture the adhesion of particle. The numerical scheme is discussed below in detail

2.3.1 Geometry

To perform a parametric study and better understand the impact dynamics, a 3D model was used instead of 2D. To save computational time, a quarter particle was created

to impact on a quarter cylinder substrate. The particle diameter was set to D = 50μm and a substrate height and radius, 25 times that of particle radius were used. As explained later, a three dimensional deformable solid element was used to create the particle and the substrate. The computational domain was partitioned to conveniently mesh them so as to reduce computational time.

2.3.2 Material

Oxygen Free High Conductivity copper (OFHC) and aluminum were used to simulate metal particle impact. Copper was used to recreate the results and validate the developed model by comparing it with the literature. The impact of a copper particle on an aluminum substrate was also modeled, these results were compared to the results reported by King *et al.* [16].

2.3.3 Material Model

The elastic response of the material was assumed to be linear and defined by the elastic modulus and the Poisson's ratio. Thermal response was described by the specific heat and thermal conductivity. Material properties for elastic and thermal response at room temperature are show in Table 2.1 [3, 15].

Table 2-1: Material properties of Copper (OFHC) and Aluminum [3, 15]. [a] indicates temperature dependent properties.

	Material Properties	Copper	Aluminum	Unit
	Density[a]	8960	2700	kg/m3
	Elastic Modulus[a]	126	65.762	GPa
	Poisson's Ratio[a]	0.335	0.3	
Plasticity Constants	A	90	148.361	MPa
	B	292	345.513	MPa
	n	0.31	0.183	
	C	0.025	0.001	
	m	1.09	0.859	
	Melting Temp	1356	930	K
	Reference Temp	298	298	K
Damage Parameters	d1	0.54	0.071	
	d2	4.89	1.248	
	d3	-3.03	-1.142	
	d4	0.014	0.147	
	d5	1.12	1.0	
	Specific Heat[a]	383	920	J/kgK
	Thermal Conductivity[a]	401	220	W/mK
	Inelastic Heat Fraction[a]	0.9	0.9	

The plastic deformation of the material was modeled using Johnson-Cook plasticity model which accounts for strain hardening, strain rate hardening and thermal softening effects. The stresses were expressed according to Von Mises plasticity model,

$$\sigma = (A + B\varepsilon_p^n)(1 + C\ln(\dot{\varepsilon}^*))(1 - (T^*)^m) \tag{2.1}$$

$$T^* = \begin{cases} 0 & \text{for } T < T_r \\ (T - T_r)/(T_m - T_r) & \text{for } T_r \le T \le T_m \\ 1 & \text{for } T > T_m \end{cases} \tag{2.2}$$

where *A*, *B*, *C*, *n* and *m* are constants dependent on the material, ε_p is the equivalent plastic strain (PEEQ) which is the scalar measure of all the components of equivalent plastic strain equivalent to Mises stress, $\dot{\varepsilon}^*$ is dimensionless effective plastic strain rate normalized with respect to reference strain rate (usually 1 s^{-1}). T^* is homologous temperature defined by equation (2) with T_m as melting point and T_r as reference or transition temperature define as the temperature at or below which there is no temperature dependence of yield stress (usually room temperature) [20].

The most important aspect during the simulation of cold spray particle impact is the possible excessive distortion of elements near contact surfaces, especially at a higher particle velocity. The main measurements to cope with this problem in ABAQUS include element distortion and material damage. Johnson-Cook damage model was put to use, which accounts for the effects of hydrostatic pressure, strain rate and temperature. The Johnson-Cook dynamic failure model is based on the value of the equivalent plastic strain at element integration points, where failure is assumed to occur when the damage parameter exceeds 1. The damage parameter, ω is given by

$$\omega = \sum \left(\frac{\Delta \bar{\varepsilon}_p}{\bar{\varepsilon}_{pf}} \right) \tag{2.3}$$

$$\bar{\varepsilon}_{pf} = \left[d_1 + d_2 \exp\left(d_3 \frac{p}{q} \right) \right] \left[1 + d_4 \ln\left(\dot{\varepsilon}^* \right) \right] \left(1 + d_5 T^* \right) \tag{2.4}$$

where $\Delta\bar{\varepsilon}_p$ is an increment in the equivalent plastic strain. $\dot{\bar{\varepsilon}}_{pf}$ is the strain rate at failure which is expressed by the failure parameters $d_1 - d_5$ measured at or below transition temperature. Here, p is the pressure stress and q is the Mises stress.

The material parameters are illustrated in the Table 2-1 [3, 15].

2.3.4 Step

Initially, the impacting process was assumed to be an adiabatic process, heat transfer was not considered based on simple estimation that the time scale is very small for any heat transfer to take place. However, a study by Schmidt *et al.* [6] suggested that the heat conduction through the substrate should be considered in most cases. Both solution procedures, dynamic explicit and dynamic temperature explicit, were examined and applied to the model in this study. The dynamic temperature explicit procedure takes into effect the thermal degrees of freedom while dynamic explicit ignores these thermal degrees of freedom assuming adiabatic process. This leads to over prediction of stresses and temperatures. Thus dynamic-temperature-explicit procedure was preferred over dynamic-explicit. Both procedures were applied, but results were found to be more realistic when dynamic temperature-explicit procedure.

The computation time was decided to be 100ns for the entire impact process for metals.

2.3.5 Contact Properties

Contact and interaction properties have a crucial role to play in impact simulation. General contact was preferred over surface to surface contact to simulate impact conditions between the spherical particle and the substrate since it is faster than contact pair algorithm and is geared towards models with multiple elements and complex topologies.

General contact also permits defining contact between many or all regions of a model with a single interaction with very limited restrictions. Contact pairs on the other hand, need more careful and separate definition of the contact surface. It enforces a lot of restrictions on the type of surfaces involved. This type of contact is usually applied to 2D models. Also general contact considers the interior elements of the part for contact while this needs to be specified separately for contact pairs.

Penalty contact, a suboption with general contact was used as it offers less stringent enforcement of contact constraints than the Kinematic Algorithm. It allows the treatment of more general types of contact. Kinematic contact, another suboption, works well in most cases but some problems with chattering contact would work more easily with penalty contact. Contact properties with Tangential behavior and Normal behavior were used. The default settings were accepted with coefficient of friction of 0.2 [2].

2.3.6 Initial and Boundary Conditions

The particle and substrate were arranged together as show in Figure 2-1(a). A clearance of 5μm was given between the particle and substrate before impact. The bottom face of the substrate was fixed in all degrees of freedom; symmetric boundary conditions were applied on the vertical faces such that they were allowed to move only in the y-direction as defined in Figure 2-1(a).

The Predefined fields tool was used to describe the initial conditions, namely Velocity and Temperature. The particle velocity U_i was varied according to the material being used.

Also the particle and substrate temperatures, T_i and T_s were predefined using this tool. These values were changed to suit possible initial conditions under which the results were expected to be acceptable.

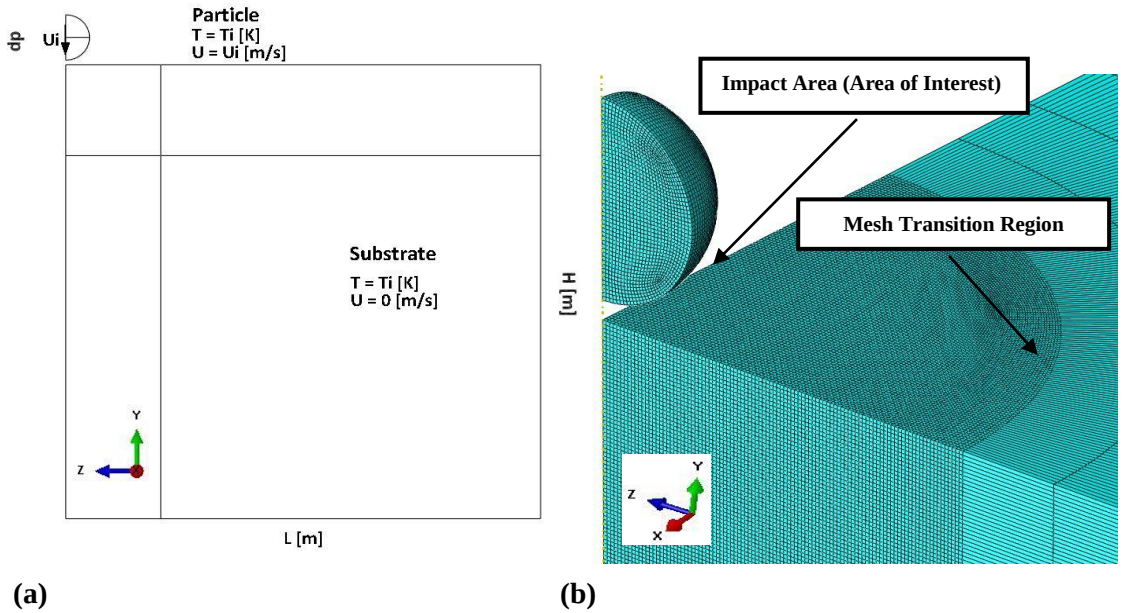

Figure 2-1: (a) Computational domain and initial boundary conditions, (b) meshing arrangement (meshing resolution of 1/50 d_p for a 50 µm particle).

2.3.7 Meshing and Element Type

Mesh plays a major role in computation and influence on the resultant output significantly. Mesh resolution dependence was investigated by varying the number of elements along the particle diameter from 50 elements to 200 elements. The results improved when the mesh size was changed from 50 elements to 100 elements, but further increase in the number of elements just added to the computation time without any further improvement in the results. Therefore, mesh density of 100 elements along the particle diameter was used for all the cases. To ensure better convergence, the element sizes at the particle substrate interface were kept the same. For computational efficiency, the mesh density was reduced away from the impact area in the substrate as shown in Figure 2-1(b).

Element type also affects the way each element in the mesh behaves during the simulation. An 8 node hexahedral explicit linear coupled temperature-displacement element (C3D8RT) was used for dynamic temperature-displacement explicit procedure while 3D stress element was used for dynamic explicit. Various combinations were experimented in addition to the element type were used such as element deletion, distortion control, reduced integration and hourglass control. It was found that distortion control was necessary for speeds higher than 500 m/s for copper.

2.4 Results and Discussion – Model Validation

The impact simulations of a copper particle on a copper substrate were carried out for two different particle velocities U_i = 500m/s and U_i = 700 m/s. Figure 2-2 shows the plastic equivalent strain (PEEQ) and the temperature profiles in the particle and substrate just before rebound. Both simulations terminated normally. The particle has a large amount of kinetic energy which is dissipated as plastic deformation and heat. Increasing the initial velocity by 40% (500m/s to 700m/s) results in 45% higher plastic strains. The increase in the strains is accompanied by 35% increase in temperatures which is evident in Figure 2-2. Maximum deformation is confined to the impact surfaces where most of the deformation is plastic. As the particle impact velocity is greater than the critical velocity, the material near the impact area is subjected to adiabatic shear instability. This instability is caused by large shear stresses on the surface in contact during impact which are large enough to accelerate the material laterally outwards. The lateral movement of the material causes the formation of the jet. The jet is that part of the material which is plastically deformed due to the pressure force generated during impact. The temperatures in these regions are high enough to cause localized melting of the particle and substrate material. Due to the

temperature rise, thermal softening effect dominates the strain rate hardening, thus the material flows forming a jet which is clearly visible in Figure 2-2.

Figure 2-3 compares the results obtained from the current model to the work of Yildirim *et al*. [15]. The maximum plastic strains and temperature in the particle and substrate for a copper particle impact on copper substrate for initial velocity of U_i = 500m/s and U_i = 700m/s are shown. As it can be seen in Figure 2-3(a), maximum strains of 3.8 for particle velocity of 500m/s and 5.6 for particle velocity of 700m/s were obtained which are significantly higher when compared to the results in Figure 2-3(b). Thus, our results were scaled down to show the deleted elements and the scale was matched to the values of results obtained by Yildirim *et al*. The under prediction of strains and temperature in results obtained from Yildirim *et al.* can be attributed to the use of shear damage in addition to the ductile damage criterion (J-C damage model). Another reason for the difference in the results is due the number of elements deleted. It can be seen that many extensively deformed elements have been deleted due to the use of shear damage thus giving lower plastic strains. When these excessively deformed elements are deleted manually from the model by reducing the strains, the particle deformation is comparable.

A similar trend has been observed with temperature distribution. While the temperature profiles at 500m/s are almost similar, those at 700m/s are over predicted. The non-colored part of the contour shows the over prediction of temperature. This can again be attributed to the number of deleted elements. Due to the use of shear damage, the non-colored elements in Figure 2-3(c) are deleted reducing the temperature range. Although temperature profiles at 700m/s are on the higher side, those at 500m/s are comparable.

When these results are compared to that in Figure 2-4 [3], we see that the plastic strains at 500m/s are in the same range. The result in Figure 2-4 was obtained without the use of shear damage and are comparable to ours. This shows the use of shear damage doesn't affect the result significantly, but only lowers the limit for element deletion giving lower strains. Thus, shear damage was not incorporated for our simulations.

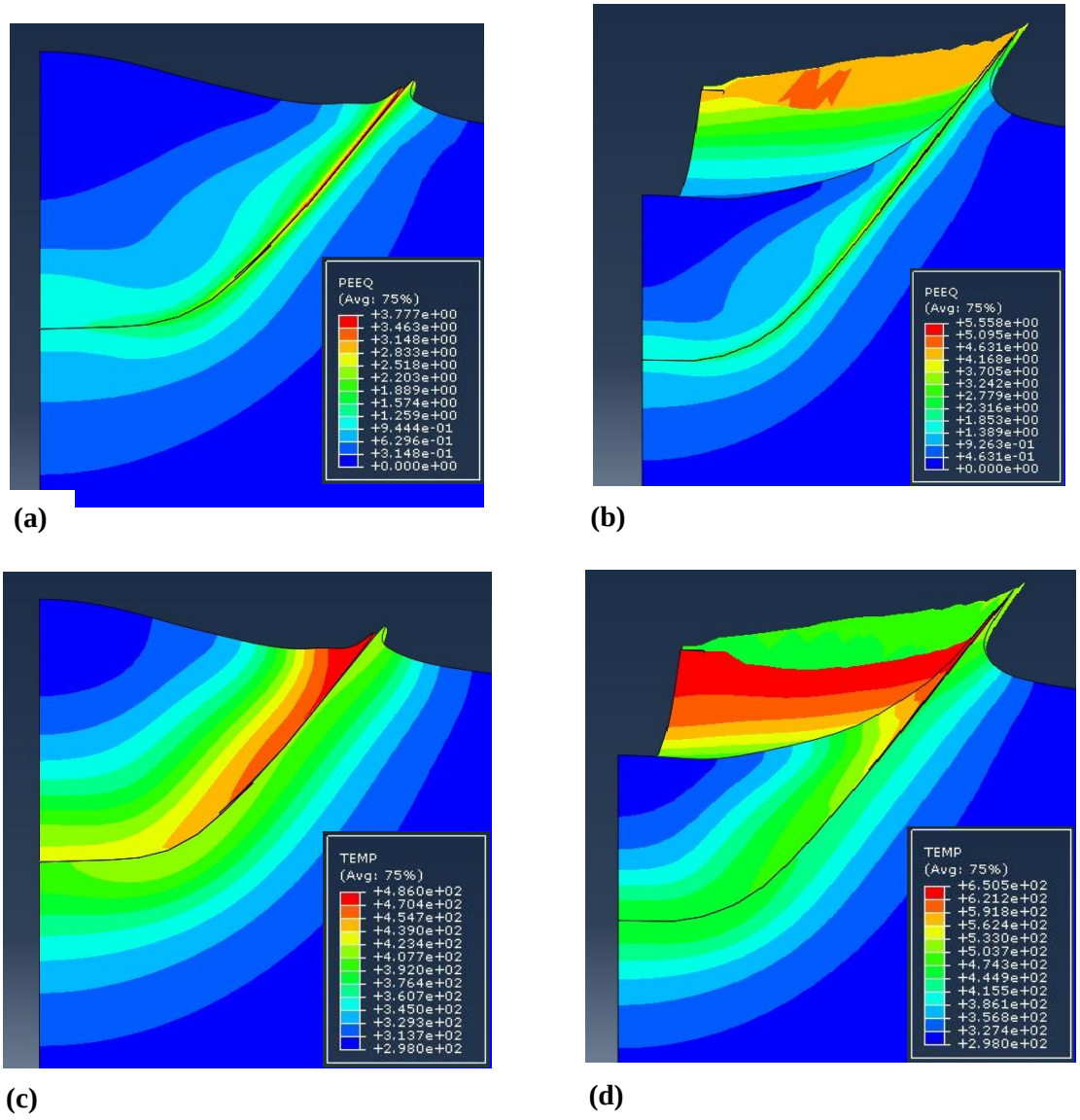

Figure 2-2: Equivalent plastic strain distribution (a) at 500 m/s, (b) at 700 m/s. Temperature distribution (c) at 500 m/s, (d) at 700 m/s for impact of Cu particle on Cu substrate.

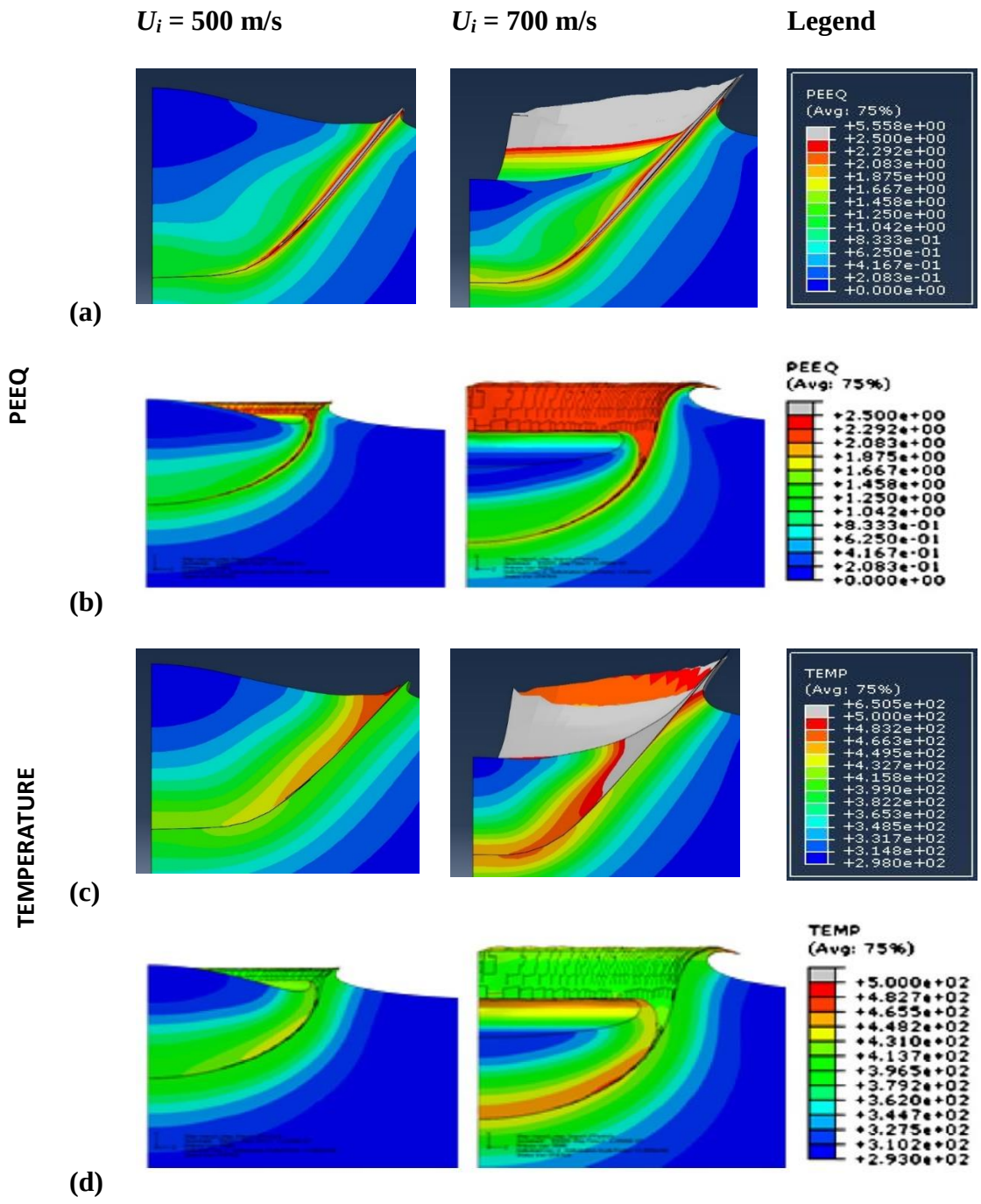

Figure 2-3: Equivalent plastic strain and temperature distribution (a), (c) Numerical results and (b), (d) Results obtained by Yildirim *et al*. for impact of Cu particle on Cu substrate.

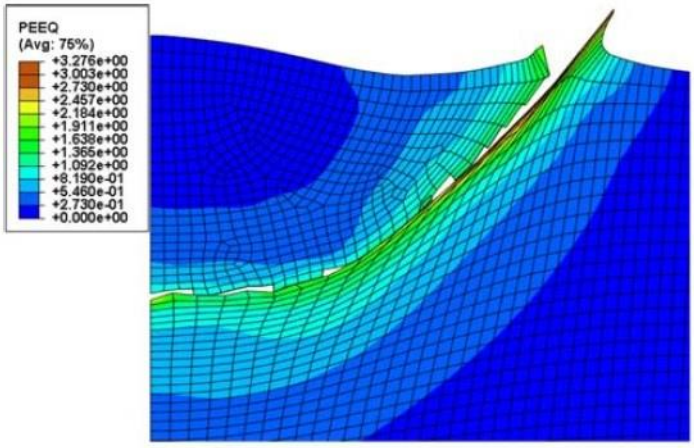

Figure 2-4: Equivalent plastic strain distribution obtained at 500 m/s by Li *et al*. 2009.

Another important aspect to consider is the deformed shape of the particle. As the particle strikes the substrate, it deforms, creating a crater in the substrate. To make a comparison between the deformed shape of the particle and substrate, another model was created using the material properties given in Table 2-1. The model consisted of a copper particle, D = 50µm, striking an aluminum substrate at U_i = 500m/s. These results were compared to the experiments conducted by King *et al.* [16]. Figure 2-5 shows the comparison between the deformed particle shape which is an SEM image of the cross section of a copper particle sprayed onto an aluminum substrate and the results obtained from the simulation. There is a good resemblance between the deformed shape of the particle during impact performed experimentally and numerically. Thus, the model gives a reasonable prediction in terms of deformed shape of the particle, the formation of the crate in the substrate and jet formation. The developed model can predict the impact of a particle over a substrate with reasonable accuracy and the results obtained are reliable. This model can be extended to predict the polymer particle impact.

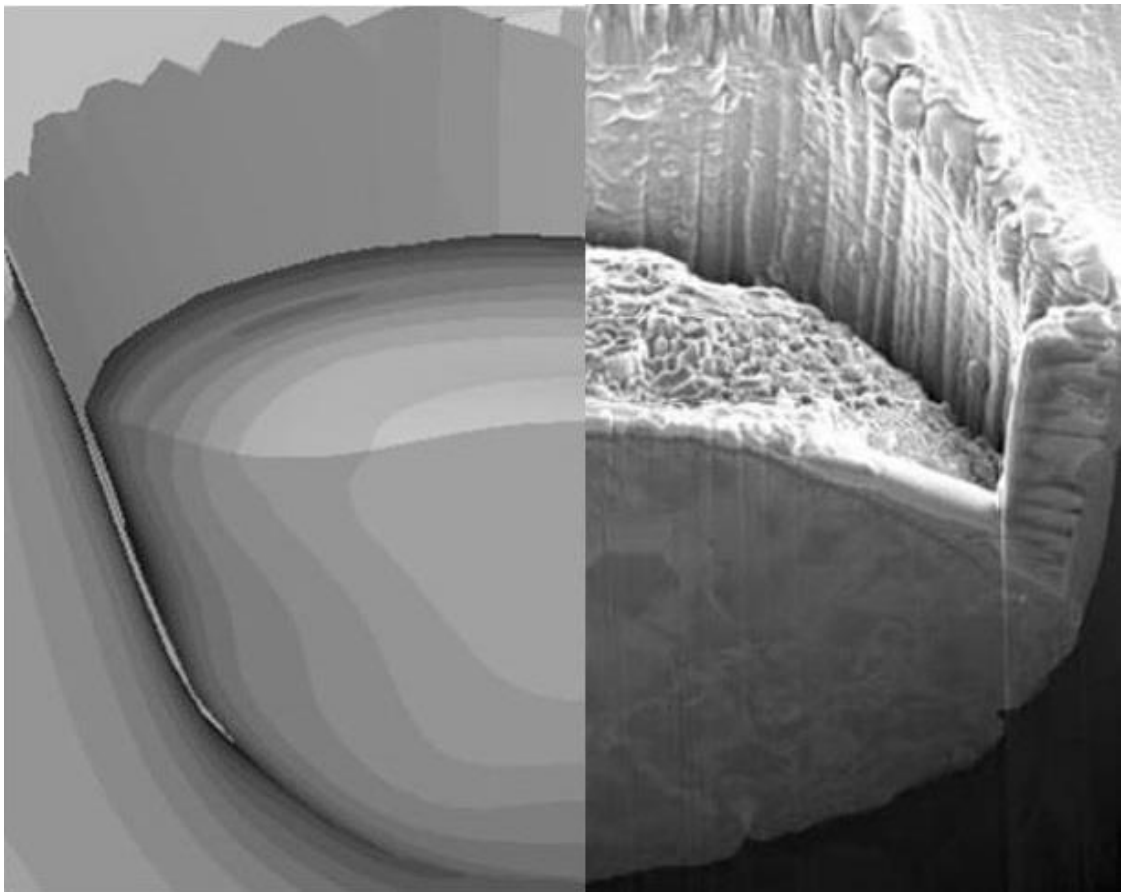

(a) **(b)**

Figure 2-5: Deformed shaped as obtained (a) from simulations, (b) from experiments by King *et al*. for impact of copper particle on an aluminum substrate at 500 m/s.

2.5 Conclusions

Metal cold spray is a well-studied topic and a lot of research has been dedicated to it. This process has plenty of industrial applications. In the past, metal cold spray has been studied numerically and experimentally. In the first part of this chapter, a detailed review of the metal cold spray process, the numerical scheme employed in the literature and the bonding mechanisms were discussed. Based on the literature review, the numerical approach employed in this study was discussed in detail. The step by step numerical modelling was described for impact of a copper particle on a copper substrate at two different initial particle velocity. The results obtained were then compared to the numerical and experimental results in the literature.

The results showed great resemblance to the numerical work done by Yildirim *et al. [15]* and Li *et al.* [3]. The under prediction of strains and temperature in results obtained by Yildirim *et al.* was because of the use of shear damage in addition to the ductile damage for copper particle impact. When further investigated, it was found that shear damage only lowered the threshold for element deletion. Also, when the results were compared to work done by Li *et al.*, similar results were obtained, even without the use of shear damage. Thus, shear damage was not incorporated in the current model.

The results obtained in this study were also compared to the experimental results from King *et al.* [16]. The final deformed shape is a great way to compare the results and to understand if the model predicts the impact dynamics accurately in addition to the numerical simulations. The deformed shape from the simulations was compared to an actual impact of a copper particle on an aluminum substrate at identical initial conditions. Aluminum being the softer of the two material, the copper particle formed a deep crater

into the aluminum substrate. The formation of jet was also evident suggesting the onset of adiabatic shear instability.

Thus, the current model predicts the impact of metal particles during cold spray deposition accurately and can be further extended to predict the impact of polymeric particles.

CHAPTER 3

MODELING OF HIGH VELOCITY IMPACT OF POLYMER PARTICLES

3.1 Introduction

In the previous chapter, metal particle impact was studied and successfully simulated. The results were in good agreement with the literature. In this chapter, we will extend the model to simulate polymer particle impact. The impact of polymer powders differs significantly from that of metals. The first part of this chapter presents an in-depth review of how polymeric materials behave under different loading conditions and the material models developed to predict this behavior are discussed. The numerical approach adopted for simulating the polymer particle impact and how it differs from metal impact is discussed in the second part.

3.2 Literature Review

One of the major issues with cold spraying of polymers is the clogging of the nozzle walls due to the preheated particles. The throat of the nozzle is the most affected. Also a suitable range for the gas stream velocity is unknown which would mean too small velocities would not cause sufficient deformation in the particle to ensure adhesion. On the other end, extreme velocities would induce large stresses on the target, large enough to overcome adhesion and strip the particles right off from the substrate [21]. An efficient approach would be to study the impact numerically and define a window of deposition before carrying out the process experimentally.

However, due to the lack of sufficient data of polymer material properties at high strain rates, it is challenging to accurately predict the behaviors of polymer particles upon

high-speed impact numerically. Recently, efforts have been made by researchers to understand the high rate and high temperature material behaviors of polymers. Colak *et al*. [22] studied the complexity of mechanical behavior of polymers and laid the basis for a constitutive model that enveloped the deformation behavior of polymers. The nonlinear rate sensitivity, unloading behavior, multiple creep and strain at zero stress were successfully modelled using the modified viscoplasticity theory based on overstress for polymeric materials. Ho and Krempl [23, 24] modified the viscoplasticity theory based on the overstress model to account for high strain rate behavior of polymers. The high impact resistance of polymers was investigated by Frank and Brockman [25]. They developed a set of unified constitutive equations that combine the nonlinear viscoelasticity and viscoplasticity, captured most of the time dependent, nonlinear response observed for polymers, including: rate-dependent and pressure dependent modulus and yield, decreasing modulus and increasing relaxation rate with increasing deformation, permanent deformation beyond yield; and strain hardening at high elongation. The time-dependent response of polymers was investigated by Kim *et al.* [26] by formulating a recursive-iterative algorithm for the combined Schapery viscoelastic model with stress dependent material properties and the Perzyna viscoplastic model based on an overstress function responses of polymers for small deformation gradient problems. The efforts of Xu and Hutchings [27] give interesting insights on the polymer particle behavior. The results suggested that smaller particles experienced greater acceleration and achieved higher final velocities than the larger particles for the same air pressure. The particle size considered in this study were 150μm and 250μm. These particles, due to their larger diameters, experienced velocities in the range of 135m/s and 120m/s respectively. This would justify

the use of initial velocity of 200m/s for a 50μm particle in the current study. Although significant melting was not observed during impact, some thermal effects might occur aiding interdiffusion and bonding between the plastically deformed particle and the substrate. Deposition onto hard aluminum substrates proved difficult for almost all spray conditions; heating the aluminum substrate gave good deposition though. The initiation of the deposition on a hard aluminum substrate represented a critical step thus requiring a thin melted layer of polymer on the aluminum substrate before the low temperature impact deposition occurred. Ravi *et al.* [28] successfully cold sprayed ultra-high molecular weight polyethylene-nano-ceramic composite on polypropylene and aluminum. Working from these advances, it is now possible to model the high-speed impact of polymeric particles on hard and soft substrate and better understand the conditions under which adhesion is possible [27].

In this study, the von Mises plasticity model with temperature and strain-rate dependence was used. The following part of the chapter describes in detail the formulation of the finite element code and the various model parameters that were integrated into the code. This is followed by a parametric study which is conducted in the next chapter to understand the impact dynamics of polymer particle impact.

3.3 Numerical Method

3.3.1 Materials

High density polyethylene was used as both particle and substrate material in most cases. Other cases for the parametric study used polycarbonate (PC), low density polyethylene (LDPE) and oxygen free high conductivity (OFHC) copper along with high density polyethylene (HDPE). The effect of strain and strain rate hardening and thermal

softening are shown in Figure 3-1 as stress versus strain plots for HDPE at various strain rates and temperatures [29]. Additional data for PC, LDPE and OFHC copper can be found in [15, 29, 30]. These data points were entered into Abaqus as temperature and strain rate dependent data.

3.3.2 Material Model

The elastic response of the material was assumed to be linear and defined by the elastic modulus and the Poisson's ratio. Thermal response was described by the specific heat and thermal conductivity. Material properties for elastic and thermal response at room temperature are show in Table 3-1 [31].

The plastic deformation of the material was modeled by using isotropic material hardening. The flow stress of the material was modeled by the von Mises plasticity model [32]. This model interprets yielding as a purely shear deformation process which occurs when the effective shear stress σ_e reaches a critical value. This effective stress is defined in terms of the principal stresses σ_i (i = 1, 2 or 3) by

$$\sigma_e = \left\{ \frac{1}{2} \left[(\sigma_1 - \sigma_2)^2 + (\sigma_2 - \sigma_3)^2 + (\sigma_3 - \sigma_1)^2 \right] \right\}^{1/2} \qquad (3.1)$$

The von Mises criterion then relates σ_e to the yield stress in tension σ_T by

$$\sigma_e = \sigma_T \qquad (3.2)$$

Table 3-1: Other material properties for High Density Polyethylene. [a] indicates temperature dependent properties.

Properties	Value	Unit
Density[a]	960	kg/m^3
Elastic Modulus[a]	0.7	GPa
Poisson's Ratio[a]	0.42	
Thermal Conductivity[a]	0.47	W/mK
Inelastic Heat Fraction	0.9	
Specific Heat[a]	1900	J/kgK

This criterion predicts that the tensile yield stress σ_T, effective shear yield stress σ_s and compressive yield stress σ_c were related by

$$\sigma_T = \sigma_c = \sqrt{3}\sigma_S \tag{3.3}$$

As shown by Equation 3.3, the classic von Mises Elastic Plastic Model relates the effective stress to yield stress in tension. However, studies have shown that when considering additional stress states such as shear and compression simultaneously, yielding can be sensitive to the hydrostatic component of stress in addition to the shear component [32]. Because the von Mises criterion does not consider hydrostatic stress, therefore, one will lose accuracy in the prediction of particle deformation. However, the von Mises model is known to give satisfactory insight into how parameter variation can affect the deformation mechanics and is used in impact dynamic simulations [33]. The computation time for the entire process was set to 500ns.

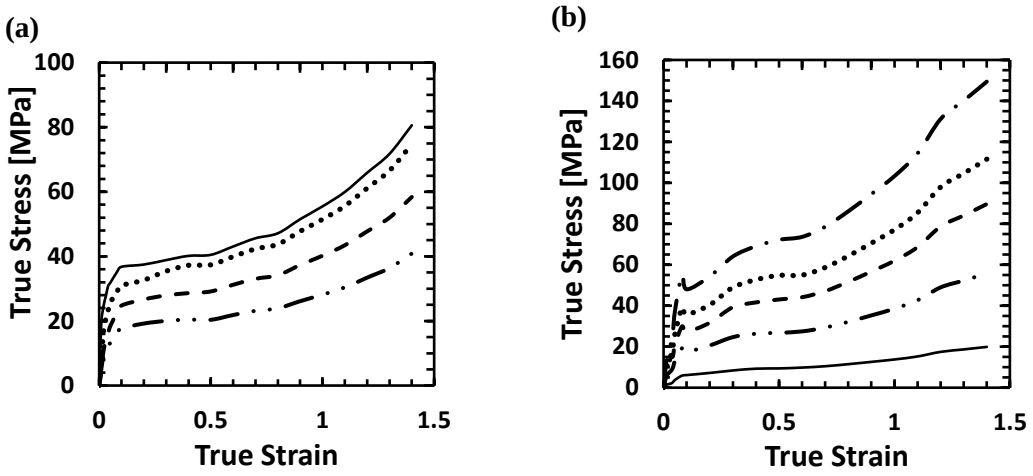

Figure 3-1: Material properties of high density polyethylene used as input into the von Mises model to simulate the particle impact. The data includes: (a) stress versus strain at a constant temperature of T_i = 298K and strain rates varying from (—··—) $\dot{\varepsilon}$ = 0.0001s^{-1}, (——) $\dot{\varepsilon}$ = 0.01s^{-1}, (·····) $\dot{\varepsilon}$ = 100s^{-1}, (——) $\dot{\varepsilon}$ = 2460s^{-1} and (b) stress versus strain at a constant strain rate of $\dot{\varepsilon}$ = 0.01s^{-1} and temperatures varying from (—·—) T_i = 198K, (·····) T_i = 233K, (——) T_i = 293K, (—··—) T_i = 323K, (——) T_i = 373K.

3.4 Conclusions

In this chapter, the uncertainty with polymeric material behavior was explained. The work from various literatures was investigated and their attempt to predict the polymer material behavior numerically was given attention. Also, the results by Xu and Hutchings [27] pointed out the smaller particles tend to act stiffer and suggested an initial particle velocity of 200m/s based on the particle diameter. The work of Ravi *et al*. [28] pointed out the problem of achieving adhesion of a polymer particle on a hard metal substrate. Ravi *et al.* also suggested that adhesion was easier for a particle impacting on an already deposited layer of soft polymer material.

Moving forward with these advances, it made sense to investigate the single particle impact during cold spray numerically. The numerical approach for polymer particle impact was discussed in this chapter. The impact of a single polyethylene particle on a semi-infinite polyethylene substrate was carried using the von Mises plasticity model using the

strain rate and temperature dependent data shown in Figure 3-1. The Lagrangian approach was adopted; 3D quarter symmetry model was generated. The bottom face of the substrate was fixed in all degrees of freedom while symmetric boundary conditions were applied on the vertical faces such that, they were allowed to move only in the y-direction. A fully coupled thermal stress analysis was conducted with 8 node reduced integration element. Mesh resolution dependence was investigated and mesh density of 100 elements across a 50μm diameter particle was employed. The initial particle velocity, U_i = 200m/s was kept constant for all cases expect when studying the effect of particle velocity. Similarly, the particle and substrate temperature were set to room temperature (T_i = 298K) for all cases expect when investigating the effect of initial particle temperature. The particle diameter was set to D = 50μm for all simulations except when the effect of particle diameter was studied. To understand the impact dynamics and polymer material behavior under various conditions, a parametric study is conducted in the following chapter. The parameters varied and the results obtained are discussed in detail.

CHAPTER 4

PARAMETRIC STUDY

4.1 Introduction

In the previous chapter, the numerical modeling of polymer particle impact was discussed in detail. The polymer particle behavior is very complex and requires further understanding. High level of sophistication is required to completely describe the polymer particle behavior. The von Mises model is known to give satisfactory results and thus it makes sense to employ the von Mises plasticity model to understand how various physical parameters affect the impact dynamics rather than trying to describe the material behavior [33].

A series of numerical simulations were performed in order to study how a number of key parameters affect the particle impact dynamics and the ability of the particle to adhere to the substrate. These parameters include particle temperature, particle size, particle impact velocity, and particle density, composition of the polymer particle, surface composition and the thickness of a polymer film on a hard metal substrate. The effect of parameter variation on impact dynamics were quantified by tracking particle temperature, deformation, plastic strain and rebound kinetic energy.

4.2 Effect of Particle Temperature

The final temperature of a metal particle after impact largely depends on the initial velocity and initial temperature. In the case of polymer particles, a large temperature spike on impact can induce local melting and polymer chain interaction and entanglement between the particle and substrate which can greatly enhance adhesion beyond van der Waals forces alone [34]. The temperature of the polymer particle will also affect how the

material behaves during the impact and after rebound as the elasticity modulus and plastic deformation are strong functions of temperature as seen previously. In Figure 4-1, the equivalent plastic strains and temperature profiles are compared for a series of initial particle temperatures varying from T_i = 248K to T_i = 348K. The substrate temperature was held constant at T_s = 298K for all cases. The particle velocity was held constant at U_i = 200m/s as shown in Figure 4-1.

In the simulations, the particle is released 5μm away from the surface travelling at the impact velocity. The initial contact occurs along the vertical axis at the bottom of the particle. A large pressure is produced at impact and it elastically and plastically deforms the particle. The elastic deformation results in energy stored in the particle which is recovered following the impact resulting in a finite rebound velocity U_r, and rebound kinetic energy, $KE_r = 1/2 m_p U_r^2$. We will utilize the rebound kinetic energy trends with parameter variations to better understand particle adhesion. The plastic deformation of the particle results in non-recoverable particle substrate deformation and a rise in temperature at the particle and substrate interface. Plastic deformation will be analyzed by plotting maximum strain values in the particle and substrate, as well as the compression ratio of the particles, $C_r = (D-D_f)/D$, where D is the initial diameter of the particle and D_f is the final compressed height of the particle. In the sections that follow we will present figures showing contours of both plastic equivalent strain and temperature for both the particles and substrate after impact. In the simulations, adhesion is not accounted for so the particles always rebound after impact. The images are a few time steps after rebound. We will also present graphs showing trends in strain, temperature, rebound velocity and kinetic energy as well as compression ratio with varying input parameters.

As shown in Figure 4-1(a) and graphs in Figure 4-2(a), the localized maximum strain induced in the particle are almost identical. When compared to the low temperature case (248K), the particle as a whole is subjected to larger average plastic strains with increasing temperature. The opposite trends are observed in the substrate. This is likely because increase in initial temperature results in the softening of the material as seen in Figure 3-1(b) which in turn leads to larger average strains throughout the particle rather than a highly localized strain at the particle substrate interface. Small spikes of high temperatures are observed in the particle near the edge of the impact zone, but most of the temperature rise in the particle can be attributed to the increase in the initial particle temperature. As seen from Figure 4-2(c), the rebound velocity and the rebound kinetic energy of the particle were reduced by 20% as the temperature was increased from 248K to 348K. These results suggest that the increase in particle temperature and its resulting softening might prove beneficial for particle adhesion even without accounting for the increase in chain mobility and entanglement during impact.

To better understand whether the particles will likely adhere to the surface, we can compare the rebound kinetic energy, KE_r directly to the work of adhesion which is defined as

$$W_{PS} = (\gamma_P + \gamma_S - \gamma_{PS})A \tag{1}$$

where A is the contact surface area between the particle and the substrate, γ_P is the surface tension of the particle, γ_S is the surface tension of the substrate and γ_{PS} is the interfacial tension between the particle and the substrate [35], which can be estimated as

$$\gamma_{PS} = \gamma_P + \gamma_S - 2\sqrt{\gamma_P \gamma_S} \tag{2}$$

The resulting work of adhesion becomes

$$W_{PS} = 2A\sqrt{\gamma_P \gamma_S} \tag{3}$$

For HDPE, $W_{PS} = 2A\gamma_P$ where γ_P = 35.7 mN/m [36]. For the impact shown in Figure 4-1, W_{PS} = 0.9nJ. This is very small when compared to the rebound KE shown in Figure 4-2. Thus we are missing some addition physics that needs to be accounted and better modeling approach is needed.

4.3 Effect of Initial Particle Velocity

The initial particle velocity or the initial kinetic energy is known to play a significant role in cold spray particle deposition. Adhesion is known to take place only if the initial particle velocity is larger than or equal to a certain velocity known as the Critical velocity which is different for different materials and condition. As, not much research has been dedicated to cold spraying of polymers, there is no thumb rule available as far as the critical velocity is concerned. Thus, the impact of a 50μm HDPE particle was simulated at particle velocities ranging between 150m/s and 250m/s. The particle and substrate temperatures were kept constant at 298K.

The equivalent plastic strain (PEEQ) and the maximum temperature distribution in the particle and the substrate just after the rebound of the particle for initial particle velocities of U_i = 150m/s to U_i = 250m/s are shown in Figure 4-3. For the range of velocities tested, the plastic deformation and the temperature of the material were found to increase with increasing particle velocity. It is evident from Figure 4-3, the equivalent plastic strains increased by almost 300% for a 100m/s increase in initial velocity of the particle. The highest deformations were confined to volumes at the particle substrate interface resulting in a significant increase of the temperature in these regions from T_{max} = 305K at 150m/s to

T_{max} = 320K at 250m/s. As the particle velocity was increased, the particle formed an increasing deep crater into the substrate. In order to quantify the particle deformation, the compression ratio or the flattening ratio is defined as the ratio of the change in particle diameter to the initial particle diameter, $C_r = (D-D_f)/D$. The compression ratio was found to increase from C_r = 0.15 to C_r = 0.25 with increasing particle velocity suggesting higher average strains in the particles with higher impact velocity. The model does not account for material melting due to temperature rise. Therefore, the energy that should have been utilized for the phase change appears in the form of large temperature spikes at the particle substrate interface where the melting is assumed to take place. Given the high speeds and the impact duration which can last less than 100ns, neglecting melting which can take seconds or minutes, may be a reasonable assumption. No visible jetting is observed for velocities as high as 250m/s. Further increase in the particle velocity causes excessive mesh distortion leading to convergence problems and thus were not included.

4.4 Effect of Particle Diameter

In previous numerical studies, mechanics of metal particle impact has been shown to strongly depend on the ratio of the kinetic energy per unit volume of the particle to the plastic strain energy density [15, 37]. This non-dimensional parameter is expressed as $\rho U_i^2/\sigma_Y$ where ρ and U_i are particle density and velocity respectively and σ_Y is the substrate's dynamic yield strength. Thus, from the above relation, the results are expected to be independent of the particle diameter if the material behavior is rate independent and the gravitational effects are negligible. Since we are dealing with micron-sized bodies, the gravitational effects can be considered negligible. However, as we can see from the Figure

3-1(a), the material behavior is highly rate dependent and thus the effect of particle size needs to be investigated.

In order to study the effect of HDPE particle size, impact of particles with diameter of 50μm, 250μm and 500μm were simulated on an HDPE substrate for an initial particle velocity of U_i = 200m/s. The contours of plastic deformation and temperature distribution in the particle and substrate are shown in Figure 4-5. Although the particle diameter is increased by a factor of 10 and the impact kinetic energy by 1000, little change in the strain field or the temperature profile is observed with increasing particle size. In Figure 4-6(d), the compression ratio C_r which can be viewed as average deformation of the particle is plotted as a function of the particle size. A monotonic growth in the compression ratio is observed with increasing particle size even as both the maximum temperatures and strains were found to demonstrate a maximum for the middle sized particle tested as shown in Figure 4-6(c) and 4-6(d). Smaller particles tend to act stiffer than larger particles due to the higher strain rates and thus higher dynamic yield strength they encounter during impact. Thus, our simulations clearly show that it is easier to deform larger particles upon impact. Adhesion, however, is a different story. The rebound velocity and the corresponding rebound kinetic energy are plotted in Figure 4-6(c) for varying particle diameter. The rebound particle velocity was found to reduce with particle size due to increase in the average strain observed in the compression ratio. The rebound kinetic energy increases with particle size due to the increase in the mass of the particle. If the particle rebound *KE* is normalized by the particle mass, the data in Figure 4-6 show that more of the incoming *KE* is dissipated as thermal energy during impact due to the plastic deformation of the particle. Unfortunately, even as more energy is dissipated for larger diameter particles, the

rebound KE still grows like the mass or $KE \propto D^3$ while the work of adhesion grows with $W_{PS} \propto D^2$. As a result, unless the rate dependent material properties result in a kinetic energy that grows slower than D^2, smaller particles will always be expected to adhere more strongly on impact.

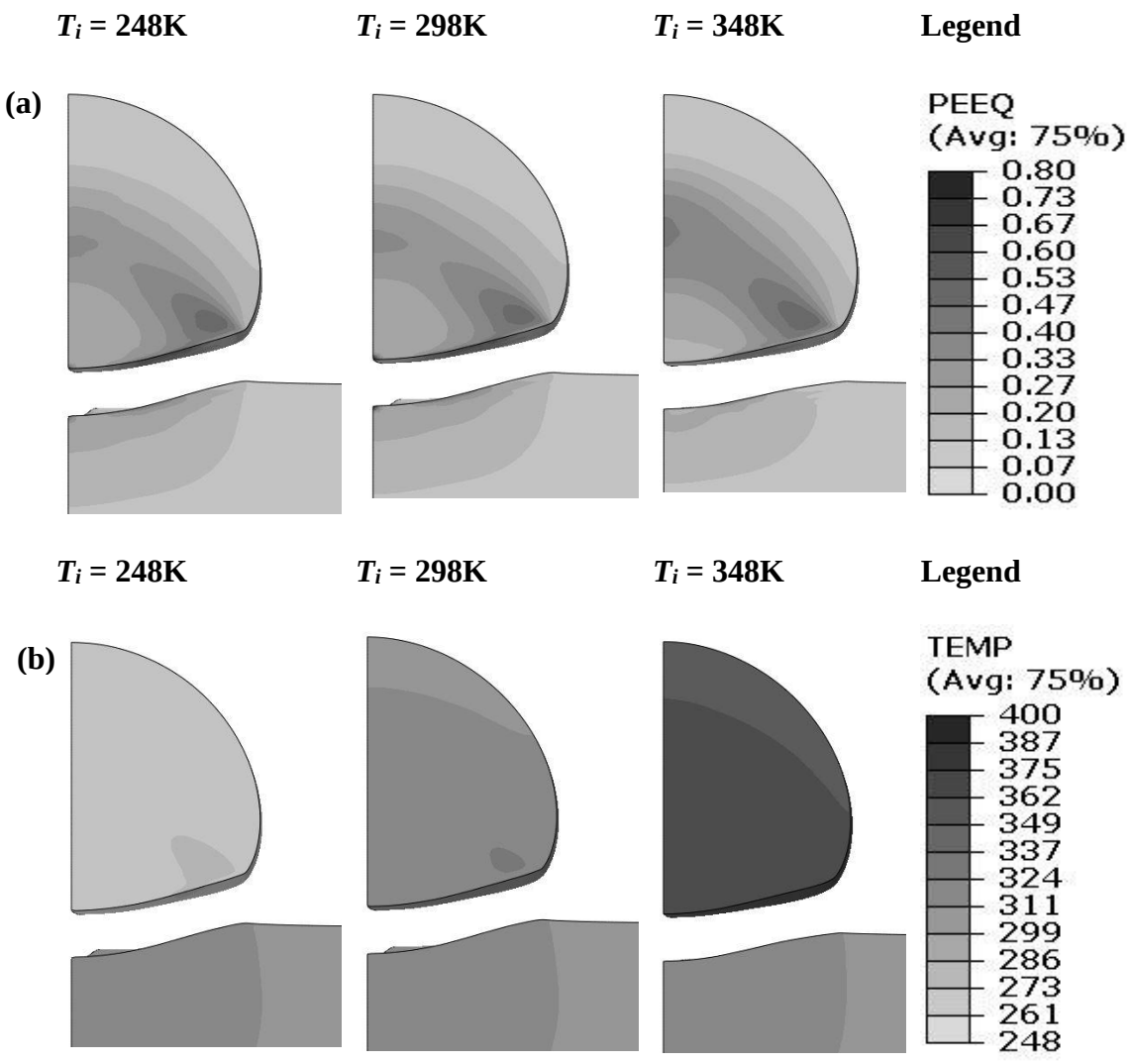

Figure 4-1: Simulation results of the final deformed state of a high density polyethylene particle impacting on a high density polyethylene substrate at a temperature T_s = 298K with an initial velocity U_i = 200m/s. The particles shown have an initial temperature T_i = 248K, 298K and 348K. Data for (a) plastic deformation (PEEQ) and (b) temperature are shown.

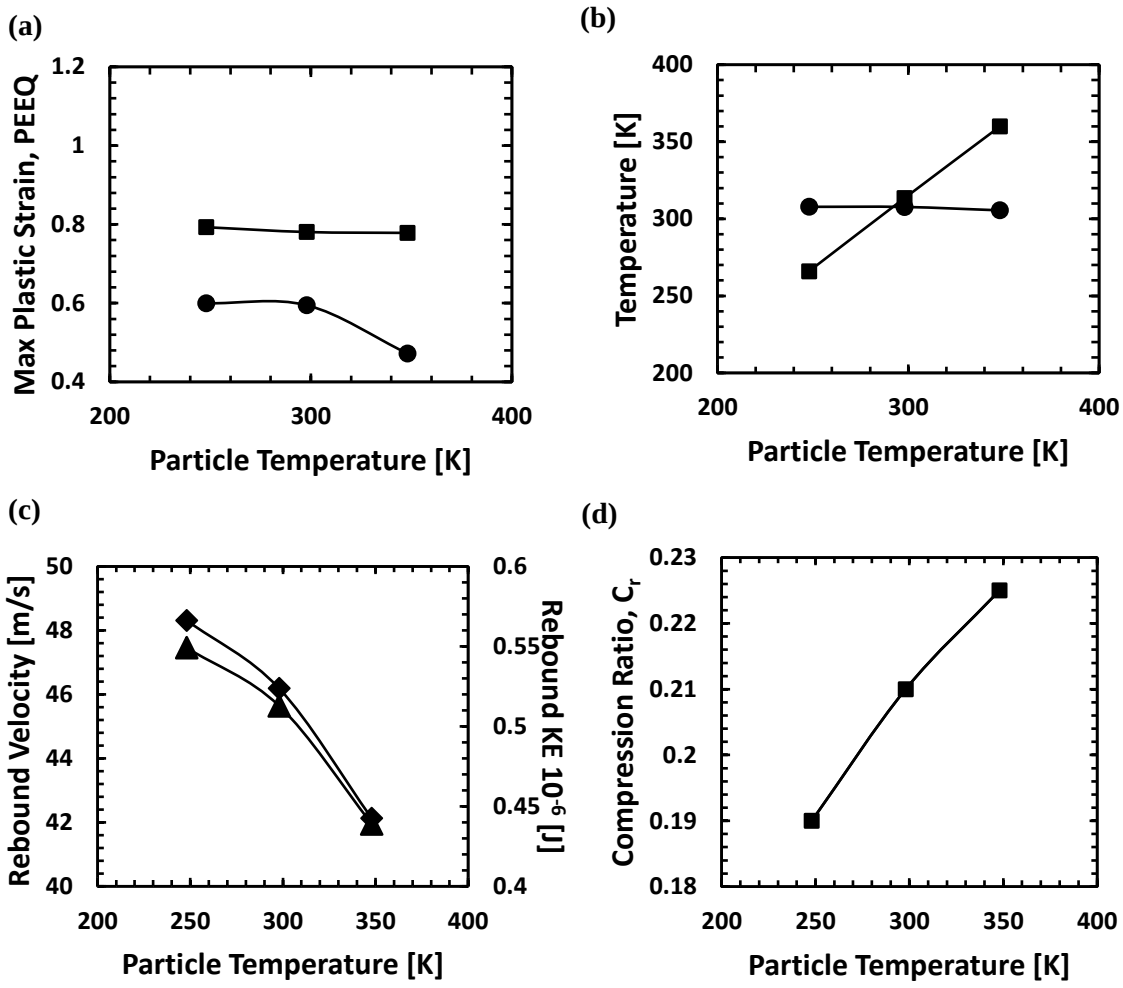

Figure 4-2: Data showing the effect of initial particle temperature on: (a) maximum plastic deformation (PEEQ) in the (■) particle and (●) substrate, (b) maximum temperature in the (■) particle and (●) substrate, (c) (▲) rebound velocity of the particle after impact and (◆) rebound kinetic energy of the particle after impact, (d) (■) the compression ratio C_r of the particle. The simulations were carried on with an initial velocity of U_i = 200m/s and initial temperature T_i = 248K, 298K and 348K.

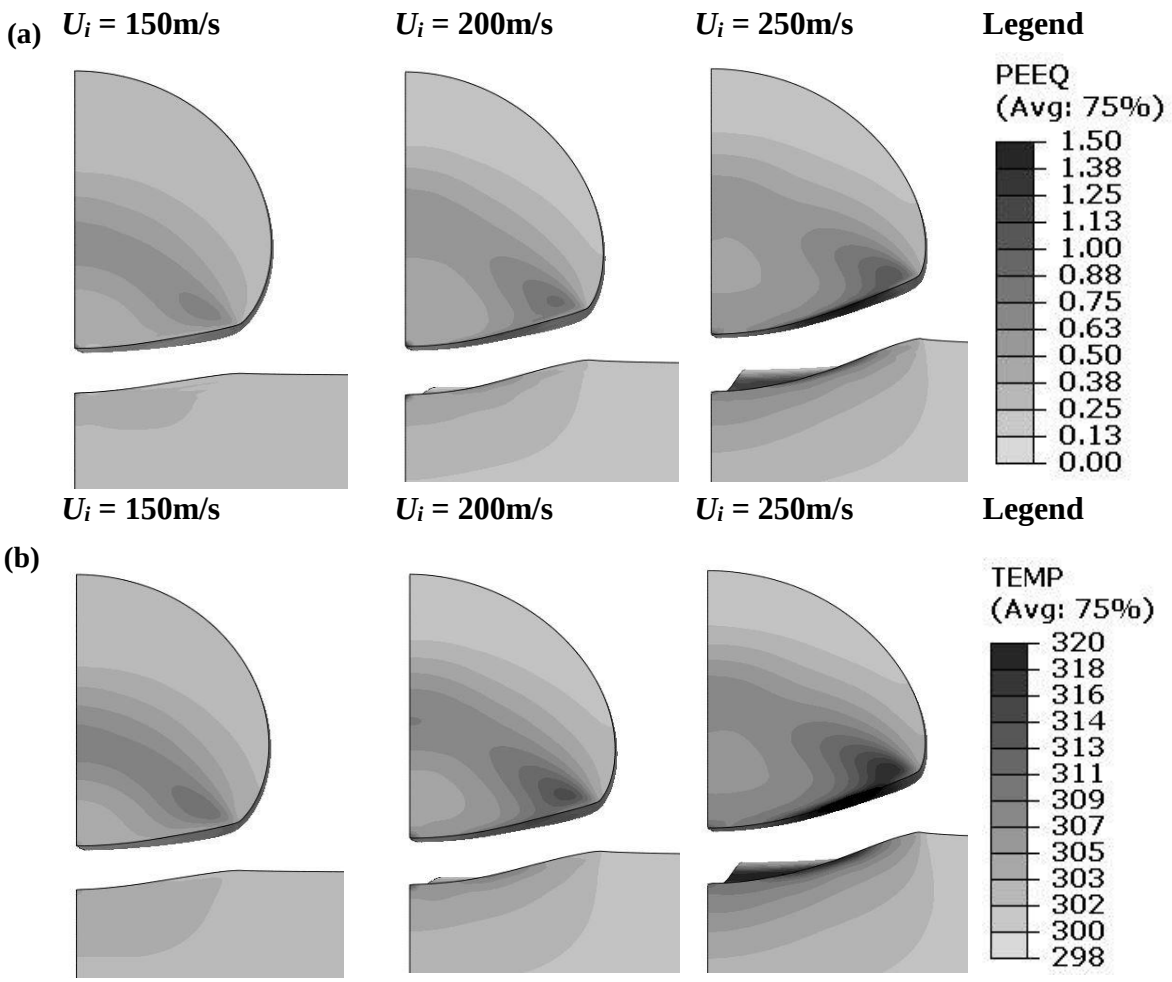

Figure 4-3: Simulation results of the final deformed state of a 50μm diameter high density polyethylene particle impacting on a high density polyethylene substrate at an initial temperature T_i = 298K. The particles shown have an initial velocity U_i = 150m/s, 200m/s and 250m/s. Data for (a) plastic deformation (PEEQ) and (b) temperature are shown.

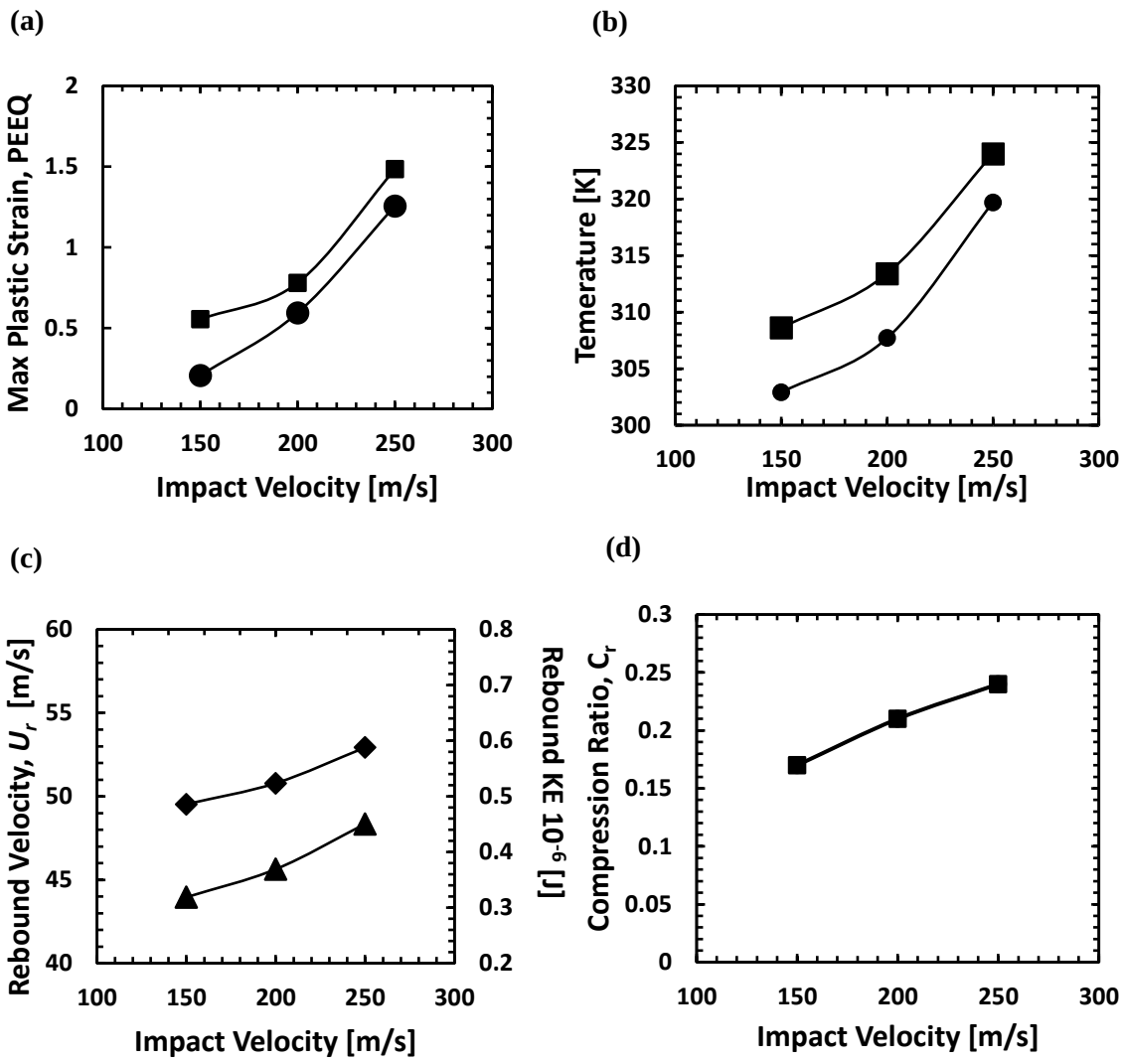

Figure 4-4: Data showing the effect of initial particle velocity on: (a) maximum plastic deformation (PEEQ) in the (■) particle and (●) substrate; (b) maximum temperature in the (■) particle and (●) substrate, (c) (▲) rebound velocity of the particle after impact and (◆) rebound kinetic energy of the particle after impact and (d) (■) compression ratio C_r of the particle. The simulations were carried on with an initial velocity of U_i = 150m/s, 200m/s, 250m/s and initial temperature T_i = 298K for 50μm particle diameter.

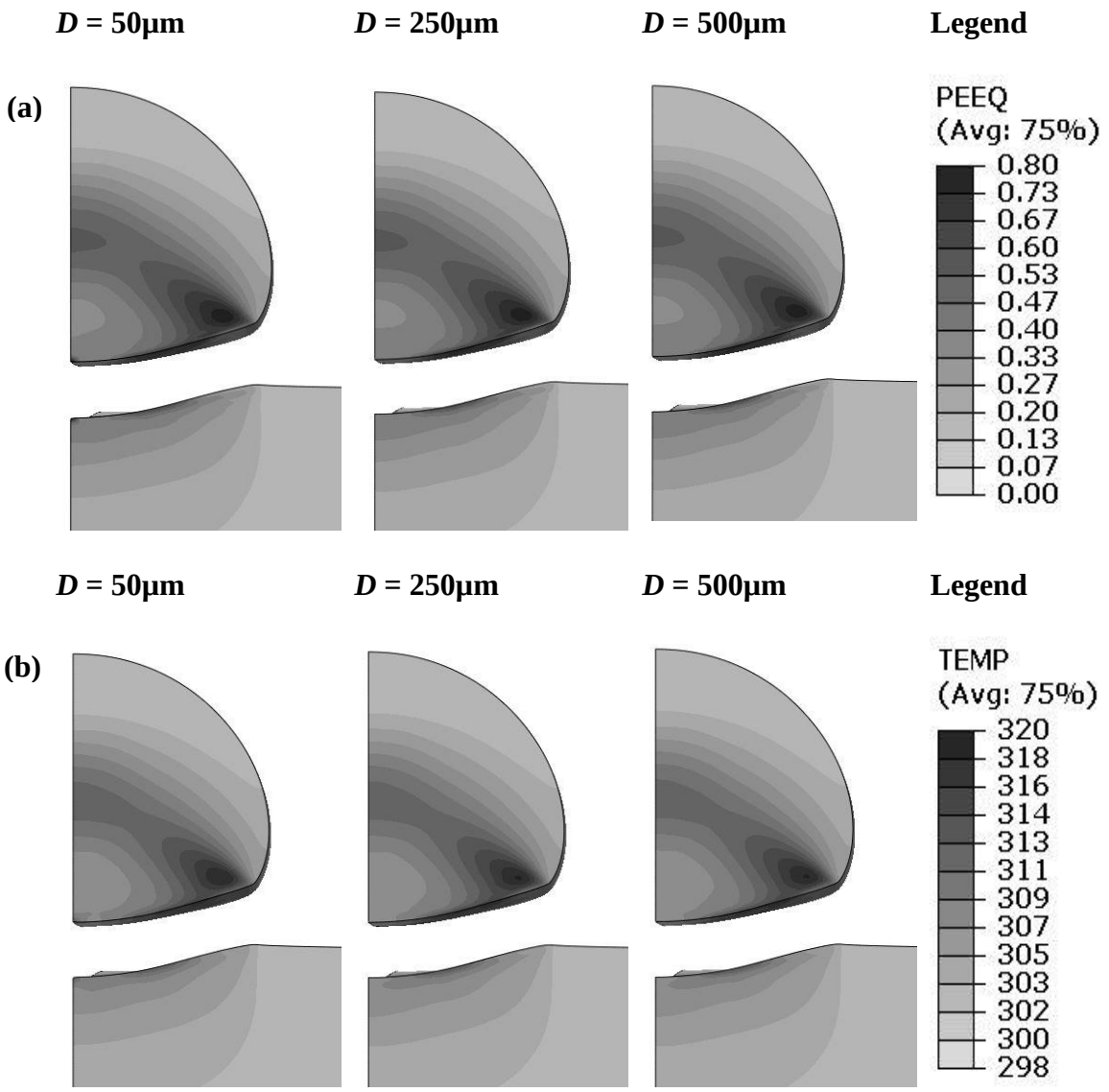

Figure 4-5: Simulation results showing the final deformed state of high density polyethylene particle impacting on a high density polyethylene substrate at U_i = 200m/s and initial temperature T_i = 298K with particle diameter D varying from D = 50µm to D = 500µm. In (a) the plastic deformation (PEEQ) and (b) the temperature variation is shown.

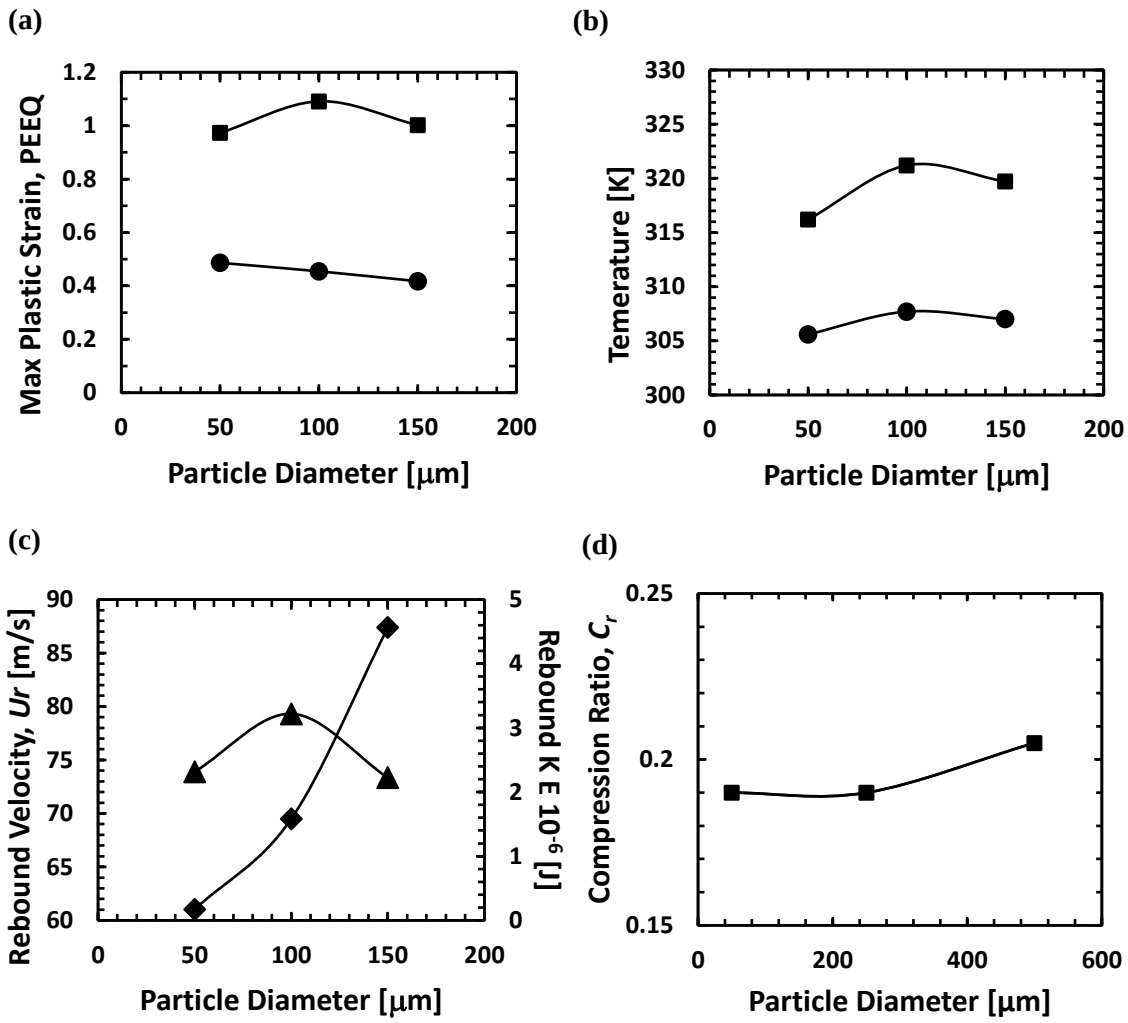

Figure 4-6: Data showing the effect of particle diameter D on: (a) maximum plastic deformation (PEEQ) in the (■) particle and (●) substrate, (b) maximum temperature in the (■) particle and (●) substrate, (c) (▲) rebound velocity of the particle after impact and (◆) rebound kinetic energy of the particle after impact, (d) (■) compression ratio, C_r of the particle. The simulations were carried on with an initial velocity of U_i = 200m/s and initial temperature T_i = 298K.

4.5 Effect of Particle Density

There are a number of applications where cold spray deposition of composite can be advantageous. For example, polymer particles loaded with copper nanoparticles would create an antibacterial coating due to the antimicrobial properties exhibited by copper [28, 38]. Alternatively, carbon nanotubes could be used to create a reinforced coating. The loading of the nanoparticle at low concentrations will have little effect on the material properties. As a first approximation, we will track the effect of nanoparticle addition as an increase in the particle density only while keeping all other properties same. As mentioned in the previous section, the dynamics of particle impact are largely governed by non-dimensional parameter $\rho U_i^2/\sigma_Y$. As a result, increasing the density of the particle is equivalent to increasing the particle velocity or reducing the yield stress. In these simulations we will investigate the effect of density on particle deformation upon impact.

HDPE particles loaded with copper nanoparticles were simulated by increasing the density of the particle to correspond to a fixed nanoparticle concentration. The density of the simulated particles was calculated to increase from 960kg/m^3, 1004kg/m^3, 1490kg/m^3 to 2905kg/m^3 as the percentage (by weight) of the copper nanoparticles was increased from 0%, 5%, 40% to 75% as shown in Figure 4-7 for composite particle impact on an unloaded HDPE substrate at U_i = 200m/s. For comparison, the pure HDPE (0% nanoparticle) impact at these same conditions is shown Figure 4-3. Increasing the density results in a larger impact kinetic energy for the particle. The percentage increase in density from unloaded HDPE to 75% copper nanoparticles by weight increases the *KE* by 300% and is equivalent to increasing the impact velocity by 175%. As shown in Figure 4-7, increasing the density results in significantly higher strains and temperatures. The dense particle forms a deep

crater in the substrate. The strain in the particle was found to increase by over 50% as the concentration of nanoparticles was increased from 0% to 75%. Interestingly, over the same range, the temperature increase in the particle was found to go down even as the peak temperatures increased substantially along the highly deformed impact surface. With large particle density, the deformation is shifted from the particle to the substrate with strains increasing from 0.5 to 1.75. Temperatures in the substrate also go up. In addition, the shape at impact shows more substantial changes and the start of jetting. The rebound velocity and the rebound kinetic energy are shown in Figure 4-8(c) against the percentage of copper. The strong increase in particle and substrate deformation leads to a reduction in the rebound velocity with increasing particle density. Most of the initial kinetic energy appears as plastic deformation and temperature rise in the substrate which causes reduction in the rebound characteristics of the particle. Although the rebound kinetic energy reduces with the increase in the density as shown in Figure 4-8(c), the drop is not enough when compared to the work of adhesion mentioned in previous section.

As mentioned earlier, increasing the particle density is equivalent to increasing the initial velocity of the particle. To confirm this, an additional case was simulated where a particle loaded with 40% copper nanoparticles impact on an unloaded substrate at 160m/s. These values were calculated by keeping ρU_i^2 = constant and using the first case (5% Cu at 200m/s) for comparison. As seen in Figure 4-7, the plastic strain profiles are identical for 5% Cu particle impact at 200m/s and 40% Cu particle impact at 160m/s. Although the strains induced in the particle are similar, the temperature in 40% Cu particle at 160m/s is less because the total initial kinetic energy input to the particle is less when compared to

the 200m/s case. Thus, it can be seen that same strains are obtained when the ratio ρU_i^2 is kept constant.

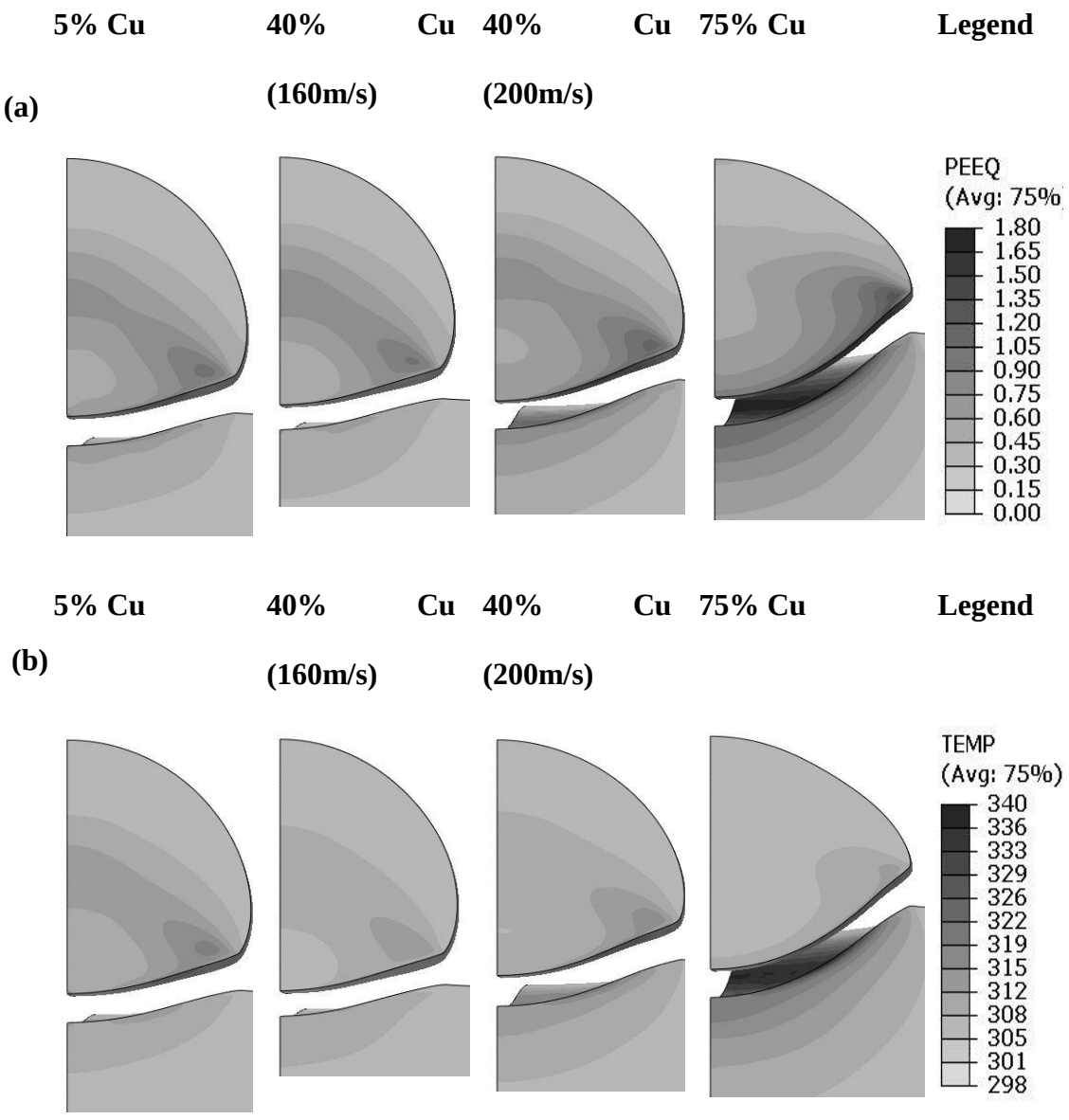

Figure 4-7: Simulation results showing the final deformed state of a high density polyethylene copper composite particle on high density polyethylene substrate with initial velocity U_i = 200m/s unless specified and initial temperature T_i = 298K with percentage weight of copper varying from 5% copper to 75% copper by weight. (a) The plastic deformation (PEEQ) and (b) the temperature distribution is shown.

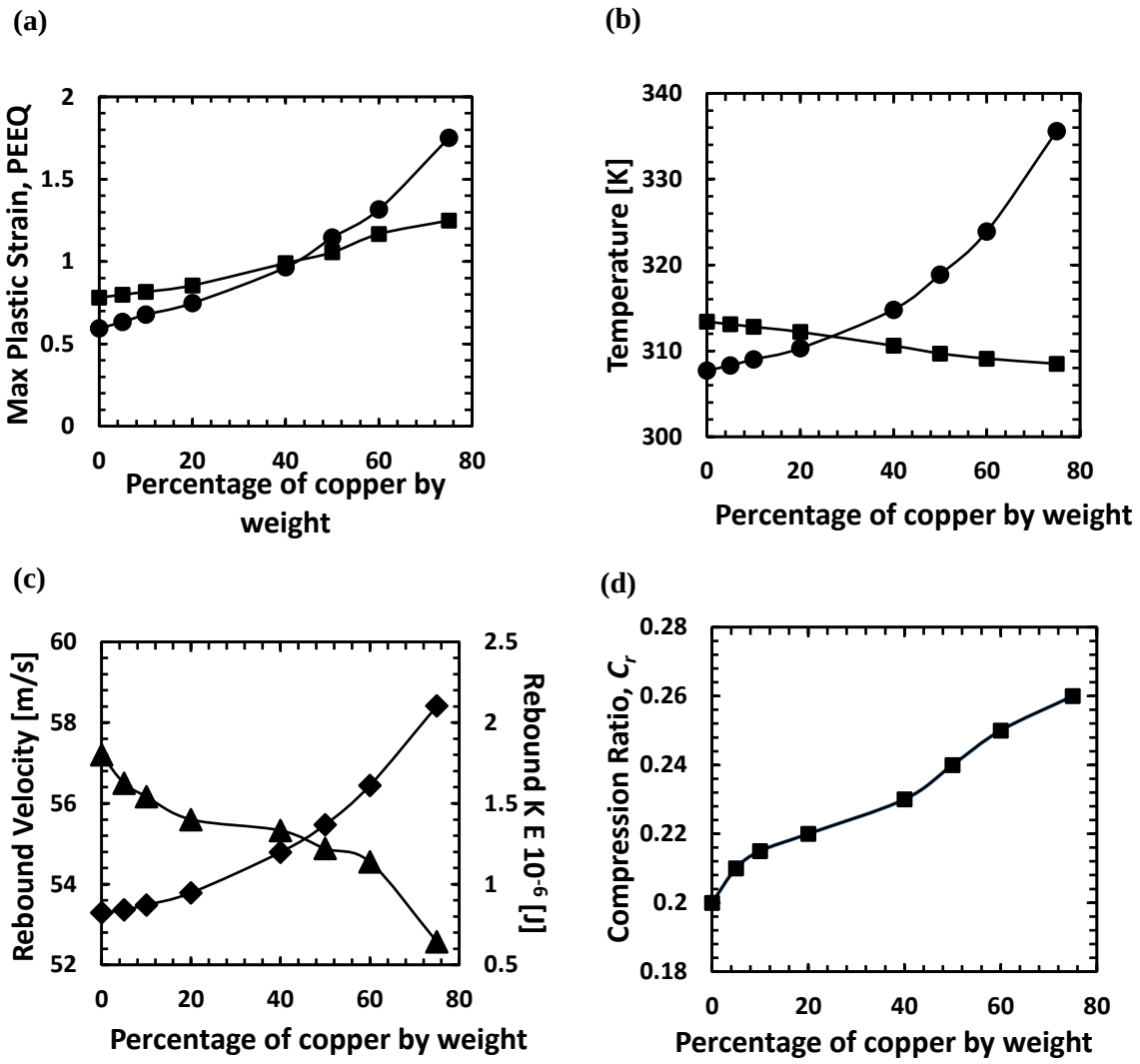

Figure 4-8: Data showing the effect of copper nanoparticle loading of high density polyethylene particle on: (a) maximum plastic deformation (PEEQ) in the (■) particle and (●) substrate, (b) temperature in the (■) particle and (●) substrate, (c) (▲) rebound velocity of the particle after impact and (◆) rebound kinetic energy of the particle after impact and (d) (■) compression ratio C_r of the particle. The simulations were carried on with an initial velocity of U_i = 200m/s and initial temperature T_i = 298K.

4.6 Effect of Substrate Material Hardness

As described earlier, the effectiveness of adhesion of the particle depends on the difference between the rebound kinetic energy and the work of adhesion, W_{ps} between the particle and the substrate. The work of adhesion is a direct function of the contact surface area, A between the particle and the substrate and also the surface tension (γ_P and γ_S) of the particle and substrate material. Changing the particle or the substrate can affect the surface tension. Additionally, the contact area is directly related to the relative hardness between the particle and the substrate. Thus, depending on how hard the substrate is compared to the particle, the surface area generated during the impact will change. The larger the deformation, the larger the work of adhesion and the less elastic strain energy stored in the particle and the substrate returning to the particle as rebound energy.

To study the effect of substrate hardness, four different substrate material were chosen: LDPE, HDPE, PC and OFHC copper. In each case, an HDPE particle was used to impact the substrate with an impact velocity of U_i = 200m/s.

As it can be observed from Figure 4.7, as the substrate modulus increases from E = 0.3GPa to E = 1.26GPa with the substrate changing from LDPE to HDPE (seen in Figure 4-3) to PC and finally Cu, the particle tends to spread laterally while simultaneously the depth of the crater in the substrate reduces. HDPE/HDPE case has minimum temperature and plastic strain, thus maximum rebound kinetic energy and velocity. As seen from the graphs in Figure 4-10, the plastic deformation and temperature distribution in the particle increases as the substrate strength increases and opposite trend is observed in the substrate. It can be seen that for HDPE/HPDE case, maximum rebound kinetic energy is observed because the strains in the particle and substrate are similar resulting in maximum elastic

stored energy. With mismatch in modulus, the strain is disproportionately distributed to the softer particle/substrate. The result is more plastic deformation in the softer of the two elements and more energy dissipation. Thus the like on like deposition is the most difficult to achieve. This phenomenon is also evident in the work done by Trenton P Bush [39].

4.7 Effect of Substrate Coating Thickness

As explained in the previous section, the substrate properties can have significant effect on the rebound characteristics of the particle. Experiments have shown that deposition on a cold metal substrate is challenging even though the modulus mismatch reduces the rebound kinetic energy. To take advantage of the mismatch while also allowing for polymer entanglement and bonding, in this section, we investigate the effect of an existing layer of coating on the deformed shape of the particle and the rebound characteristics. For this case, an HDPE particle is used to impact on a hard copper substrate with a thin coating of HDPE with the same material properties as the impacting particle. The coating thickness was varied from 2.5µm to 250µm coating. Beyond 100µm the results were equivalent to an infinitely thick HDPE film/substrate.

The particle shape after impact along with the contours of the plastic deformation and temperature distribution in the particle and the coating are shown in Figure 4-11. For comparison, the value for HDPE particle impact on copper substrate can be found in Figure 4-10 and have been included in Figure 4-12 for comparison. The effect of coating thickness on particle rebound velocity and rebound kinetic energy can be studied from Figure 4-12(c). Although the plastic strains in the particle and substrate are half with a 2.5µm coating when compared to impact on pure Cu substrate, a 15% reduction in the rebound velocity is observed. While for 5µm to 20µm coating a similar rebound velocity compared to pure

Cu was observed. For thicknesses beyond 20μm, increase of the rebound velocity towards the result for pure HDPE was found. This reduction in the velocity can be attributed to the large deformations in the particle and plastic deformations produced in the thin film coating as seen in Figure 4-11. The particle, upon impact tries to deform the thin coating thus using up most of its initial kinetic energy. This energy appears in the form of plastic deformation and the temperature rise in the particle and the coating. For a coating thickness less than 20μm, the particle with a velocity of 200m/s has enough energy to deform almost the entire thickness of the coating plastically. The hard copper substrate beneath the coating further amplifies the plastic deformation of the coating by 3 times as compared to HDPE/HDPE case, thus generating a large shear stress in the coating during impact. Once the thickness becomes more than 20μm, the effect of the underlying Cu substrate is minimized. Thus having a very thin coating of the softer of similar material improves deposition on a hard substrate. This could be useful for practical applications where a thin coating can be added to aid adhesion for the succeeding layers. The current model can be used as the first step for multiple particle impacts where the first particle adhesion is hard and it gets easier once an initial coating has formed.

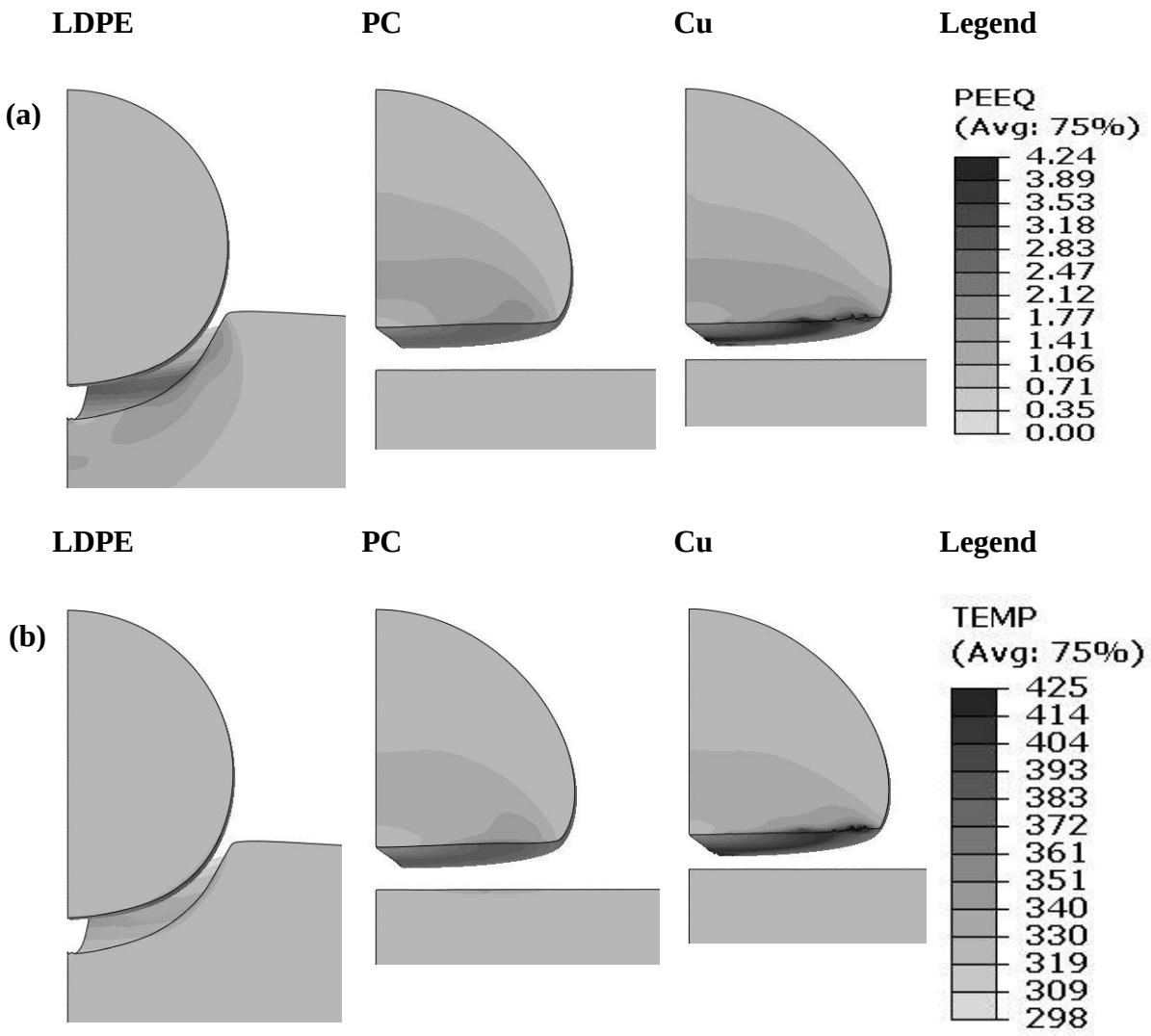

Figure 4-9: Simulation results showing the final deformed state of a high density polyethylene particle on a low density polyethylene (LDPE) substrate, polycarbonate substrate and Cu substrate with initial velocity U_i = 200m/s and initial temperature T_i = 298K. (a) The plastic deformation (PEEQ) and (b) the temperature distribution is shown.

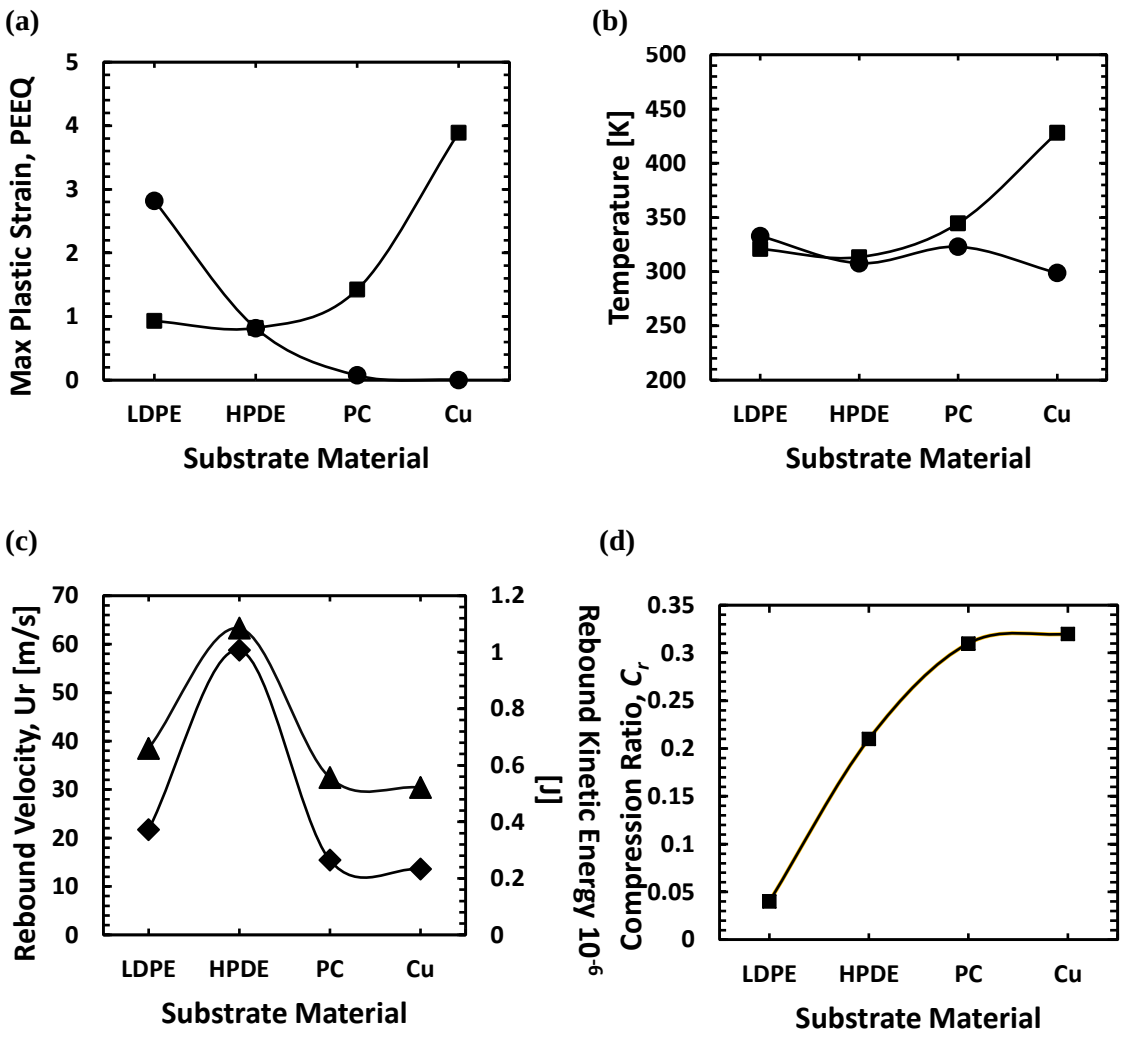

Figure 4-10: Data showing the effect of substrate hardness on: (a) maximum plastic deformation (PEEQ) in the (■) particle and (●) substrate; (b) maximum temperature in the (■) particle and (●) substrate, (c) (▲) rebound velocity of the particle after impact and (◆) rebound kinetic energy of the particle after impact and (d) (■) compression ratio C_r of the particle. The simulations were carried on with an initial velocity of U_i = 200m/s and initial temperature T_i = 298K.

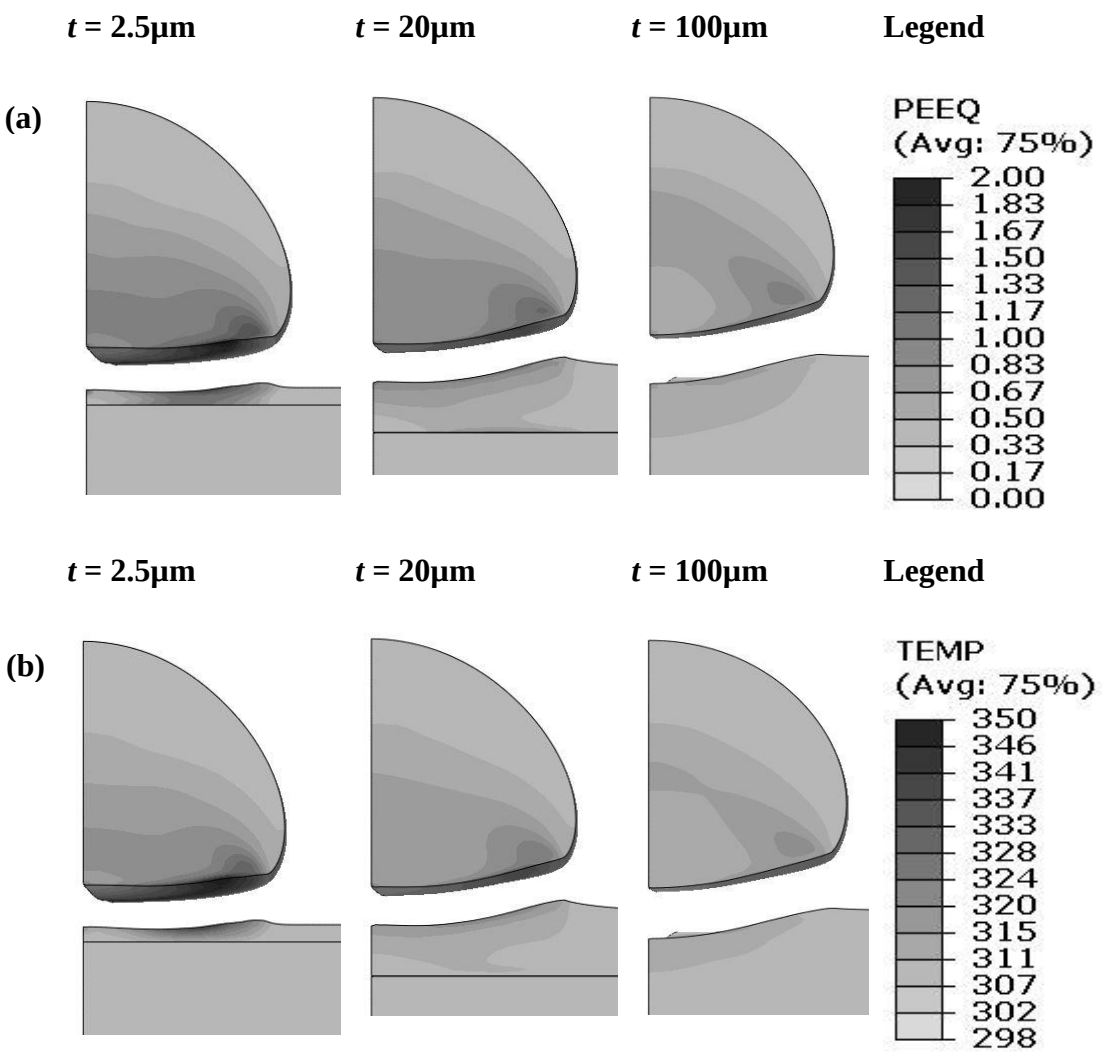

Figure 4-11: Simulation results showing the final deformed state of high density polyethylene particle impact on a copper substrate with a coating thickness t = 2.5µm, t = 20µm and t = 100µm with initial velocity U_i = 200m/s and initial temperature T_i = 298K. (a) Particle deformation (PEEQ) and (b) the temperature distribution is shown.

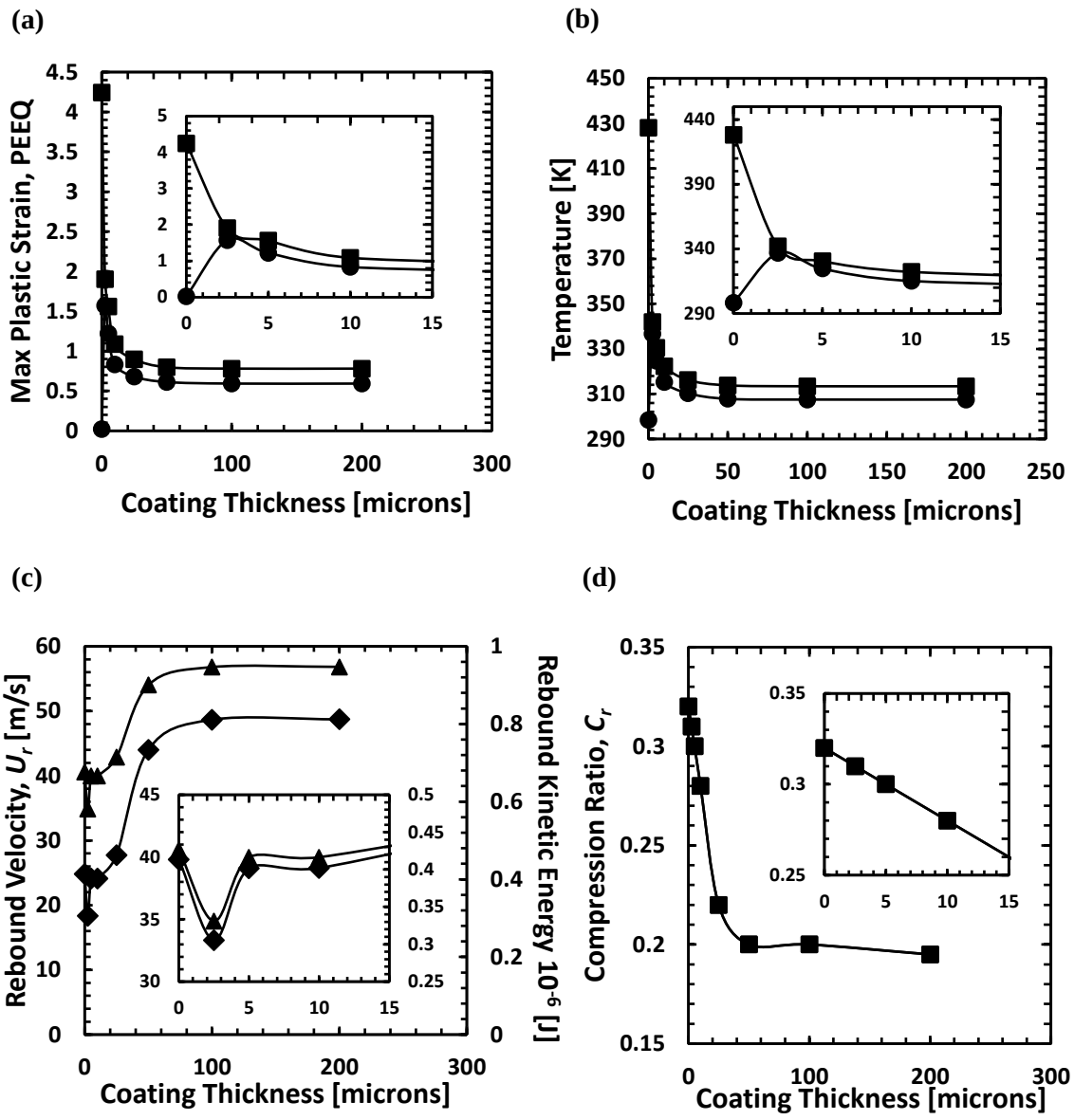

Figure 4-12: Data showing the effect of thickness of high density polyethylene coating on copper substrate on: (a) plastic deformation (PEEQ) in the (■) particle and (●) coating, (b) temperature in the (■) particle and (●) coating, (c) (▲) rebound velocity of the particle after impact and (◆) rebound kinetic energy of the particle after impact and (d) (■) compression ratio, C_r of the particle after impact. The simulations were carried on with an initial velocity of U_i = 200m/s and initial temperature T_i = 298K.

4.8 Conclusions

The initial temperature of the particle was found to play a significant role during particle impact. The increase in the initial temperature resulted in high overall deformation of the particle. The maximum strains were found to be the same for all entire temperature range but the average strain in the particle, which was considered in terms of the compression ratio of the particle, C_r increased with temperature. At the same time, the strains in the substrate did not show any significant changes due to the temperature rise of the particle except for the highest particle temperature where the strains in the substrate dropped because the particle was not hard enough to deform the substrate. The rebound characteristics of the particle also diminished with increasing temperature which suggested that softening of the particle material could prove useful for bonding.

The effect of the particle size was investigated by simulating the particle impact for three different particle diameters. The larger particles were found to deform easily due to the fact the smaller particles encounter higher strain rates and higher dynamic yield strength thus affect stiffer. It was discussed that although larger particles tend to have higher deformation, the rebound kinetic energy with which the larger particles leave the substrate is always higher mainly due to higher mass. Thus, smaller particles are expected to adhere more strongly on impact.

The damage parameter $\rho U_i^2/\sigma_Y$ which is independent of the particle size, was found effective in quantifying the effect of density of the particle during impact. The increase in density was also approximated as loading of the copper nanoparticles. An increase in the particle density was found to reduce the deformation in the particle while forming a deeper crater into the substrate. Highest deformations were observed in the substrate with

increasing particle density. Using the damage parameter above, it was also discussed that increasing the density was equivalent to increasing the particle velocity or the initial kinetic energy. This case was also simulated; the hypothesis was proved to be true.

The hardness of the substrate played an important role for adhesion of the particle. The harder substrate deformed the particle more resulting in a higher surface area for adhesion. Different materials for substrate were selected and impact for HDPE particle in LDPE, PC and Cu were simulated. It was observed that adhesion was least likely when the mismatch between the particle and substrate material was the least (same material). The higher the mismatch, the more part of the particle or substrate deforms plastically thus giving away the least amount of energy to the particle to rebound.

To take advantage of the mismatch and also to allow polymeric chain entanglement and bonding, the effect of an already deposited layer of HDPE material on a hard Cu substrate was studied. The thickness of the coating was varied over a range. It was found that the presence of a thin film aided in bonding of the particle. The particle with sufficient energy deformed the film plastically. In addition, the hard Cu substrate beneath further amplified the deformation in the film and the particle thus giving away the least possible energy to the particle to rebound.

CHAPTER 5

SUMMARY AND CONCLUSIONS

In this thesis, a numerical investigation of the high velocity impact of a micron-scale polymeric particles are presented. The major goal of this work has been to investigate the impact dynamics of a single particle impact and the various physical parameters that affect the impact. To this end, the finite element method has been used and the following physical parameters have been considered: initial particle temperature, particle size, the particle density, relative hardness of the particle compared to the substrate and the effect of an already deposited layer thickness. A velocity range from 150m/s-250m/s have been considered and the effect of the above mentioned process parameters on the outcome of the impact have been characterized by tracking the particle temperature, deformation, plastic strain and rebound kinetic energy.

Earlier, a great deal of emphasis has been given to metal particle impact, especially copper, aluminum and titanium alloy. These materials, due to their ductile behavior and relatively low strength, are greatly preferred for cold spraying application. Abundant research material is available for impacts of copper and aluminum materials and the applications are numerous. In this work, importance is given to a novel cold spray process that utilizes polymer powder. Copper and aluminum were used initially to validate our model against the numerical and experimental results in the literature. Later, numerical analysis for polymer particles was studied in detail for various impact velocities. It was shown that, as the impact velocity increases, the particle experiences more severe deformation and penetrates more into the substrate, accompanied with significant

temperature rise at the particle-substrate interface. The largest recorded deformation and temperature spikes were found around the particle-substrate interface.

The impact of a single polyethylene particle on a semi-infinite polyethylene substrate was carried using the von Mises plasticity model using the strain rate and temperature dependent data shown in Figure 3-1. The Lagrangian approach was adopted; 3D quarter symmetry model was generated. The bottom face of the substrate was fixed in all degrees of freedom while symmetric boundary conditions were applied on the vertical faces such that, they were allowed to move only in the y-direction. A fully coupled thermal stress analysis was conducted with 8 node reduced integration element. Mesh resolution dependence was investigated and mesh density of 100 elements across a 50μm diameter particle was employed. The initial particle velocity, U_i = 200m/s was kept constant for all cases expect when studying the effect of particle velocity. Similarly, the particle and substrate temperature were set to room temperature (T_i = 298K) for all cases expect when investigating the effect of initial particle temperature. The particle diameter was set to D = 50μm for all simulations except when the effect of particle diameter was studied.

In the simulations presented earlier, the particle was allowed to impact the substrate, the initial contact occurring along the vertical axis at the bottom of the particle. Due to high impact velocities, large pressure was produced and it deformed the particle elastically and plastically. The elastic deformations were stored as recoverable elastic energy which was recovered following the impact in a finite rebound velocity U_r, and rebound kinetic energy, $KE_r = 1/2 m_p U_r^2$. The plastic deformation and the temperatures in the particle and substrate were analyzed by plotting the maximum plastic equivalent strains (PEEQ) and the temperature profiles. The average deformation in the particle was

presented in terms of the compression ratio C_r. The figures with the plastic deformation and temperature contours were presented followed by the graphs with the trends in maximum strain, temperature, rebound velocity and the rebound kinetic energy, and the compression ratio with varying input parameters.

The effect of initial particle temperature was studied while varying the initial temperature of the particle from T_i = 248K to T_i = 348K and keeping the substrate temperature T_s = 298K. The localized strains induced in the particle at various initial temperatures were almost identical. However, the particle as a whole was subjected to larger average strains with increasing temperature which was evident from the compression ratio C_r while the deformation in the substrate decreased with increasing particle temperature. Also a drop of 14% in the rebound velocity and 21% in the rebound kinetic energy was observed. Thus, increasing the particle temperature and its resulting softening would prove beneficial for particle adhesion. The initial kinetic energy or the initial particle velocity tends to play a great role in adhesion of the particle and thus its effect was studied by varying the particle velocity from U_i = 150m/s to U_i = 250m/s. Increasing the initial velocity greatly increasing the plastic deformation the particle is subjected to. Similar trends were observed with temperature. However, the rebound velocity and the rebound kinetic energy increased with the increasing initial velocity due to the fact that the current model does not account for melting of the particle. Thus the part of the initial kinetic energy which should have been used for melting of the particle appears in the form of rebound velocity. Due to highly strain rate dependent behavior of polymers, the effect of particle size needed to be investigated. The particle diameter was varied from D = 50μm to D = 500μm and keeping the particle velocity U_i = 200m/s and temperature T_i = 298K. Particle

diameter did not affect the particle deformation or temperature profiles significantly. However, a monotonic growth in the compression ratio C_r was observed which indicated the larger particle deformed easily. But from adhesion point of view, because the kinetic energy grows like the mass of the particle or its volume, $KE \propto D^3$, while the work of adhesion grows with the cross sectional area, $W_{PS} \propto D^2$, it was found that small particles will always be expected to adhere more strongly on impact.

Cold spraying of composite materials was found to have plenty of applications. Thus to see the effect of addition of copper nanoparticles, the density of the particle was increasing keeping all other properties same as a first approximation. The particle density was varied from 960kg/m^3, 1004kg/m^3, 1490kg/m^3 to 2905kg/m^3 as the percentage by weight the copper nanoparticles was increased from 0%, 5%, 40% to 75% and the impacts were studied at particle velocity U_i = 200m/s and temperature T_i = 298K. Increasing the particle density resulted in a larger initial particle kinetic energy thus inducing significantly higher strains and temperatures. Although the strains in the particle increased by 50% over the increase in density by 75% by weight of copper, the temperatures recorded decreased as the density increased. As the particle became denser, more deformation was observed in the substrate followed by higher temperatures compared to the particle forming a deep crater into the substrate. Although the rebound kinetic energy increased with particle density, owing to the larger plastic deformation experienced by the particle and the substrate, the rebound velocity was found to decrease. Another interesting result found was that increase in particle density is equivalent to increase in the initial particle velocity. This was investigated by simulating the impact of a 40% copper nanoparticle loaded HDPE particle at U_i = 160m/s and comparing the results to the impact of a 5% copper nanoparticle

loaded HDPE particle at U_i = 200m/s. The results obtained showed striking similarity in terms of the deformed shape, strains induced and the temperature rise.

The substrate material plays an important role when it comes to adhesion of the particle because the relative hardness of the substrate is an important factor to consider. The effect of substrate hardness was studied by impacting an HDPE particle on four different substrate materials: LDPE, HDPE, PC and Copper at U_i = 200m/s. The substrate strength increased from E = 0.3GPa to E = 1.26GPa as the material was changed from LDPE to HDPE to PC and finally to Copper. It was found that best results were obtained when there was a mismatch between the particle and substrate material strength. For example, the HDPE/HDPE case resulted in the minimum plastic strains and temperature thus resulting in highest recorded rebound velocity and energy. Any other case, for example HDPE/LDPE case, the particle deformed the substrate forming a deep crater and the strains and temperature recorded were high in the substrate accompanied with a drop in the rebound velocity and energy of the particle while for HDPE/PC, the particle deformed with very little deformation in the substrate. The temperatures in the particle were high due to large plastic deformations. The rebound velocity was also found to be less than that compared to the HDPE/HDPE case. Thus a mismatch in the modulus proves beneficial for adhesion.

The effect of having a modulus mismatch was further exploited by simulating the impact of an HDPE particle on a hard copper substrate with a thin HDPE film. The simulations were carried with an HDPE particle impacting the copper substrate with a thin film and varying the film thickness from t = 2.5μm to t = 250μm. Although the plastic strains in the particle and substrate for a 2.5μm thin film were only 50% when compared

to no film (impact on copper substrate), the rebound velocity was found to reduce by 15%. This reduction was due to the large deformations in the particle and the plastic deformations produced in the thin film coating which led to development of enormous shear stress. Thus, most of the particle energy was dissipated in the form of plastic deformation and temperature rise in the particle and the thin film. This effect diminished as the coating thickness approached t = 20μm, beyond t = 20μm the particle behaved as if impacting on an infinite HDPE substrate. Thus, having a very thin coating of a softer or similar material will improve deposition on a hard non-polymer substrate.

Although these results give satisfactory insight about the impact dynamics of polymers and the various factors affecting the impact behavior, the current model still lacks to account for many phenomena such as melting of the material, adhesion of the particle to the substrate and polymer chain interactions and entanglements between the particle and the substrate. More accurate models that can account for these phenomena and give better predictions for polymer particle impact are needed and this study can be further extended with more sophisticated modeling approach.

CHAPTER 6

FUTURE WORKS

In the current work, the metal particle impact model has been created and validated against the numerical and experimental results found in the literature. A novel cold spray technique for polymers has been investigated and a single polyethylene particle impact has been simulated. The effect of velocity and temperature of the impacting particle have been discussed by treating them independently from one another. In order to understand the impact dynamics of polymeric particles and how polymers behave under different loading conditions, a number of numerical simulations were carried where the process parameters mentioned earlier were varied. Current work can be extended in a number of ways as recommended below.

In the current work, the von Mises plasticity model was used to predict the behavior of polymeric materials. Although this model is known to give satisfactory results, the polymeric material behavior is not accurately predicted at higher strain rates or high temperature. The effect of hydrostatic forces is not accounted for in this model. Also, the time dependent creep and relaxation behavior, and other phenomenon that are exhibited by the polymers is not accounted in this study. It the future, the current model can be extended to develop a better material model which can predict the polymer material behavior with greater accuracy.

The cold spray process consists of coating build-up by sequential impact, deformation and bond of many particles. Therefore, formation and properties of a deposited layer are not affected by the impact behavior on a single particle, but also by subsequent impact events. One such case was simulated earlier where a single particle impact on an

already deposited layer of similar material. This case, although a good approximation for multiple particle impact, neglects the surface roughness, the deformation, the temperature rise and the stresses contained in the particle before the next particle impact. Therefore, the current model can be extended to simulate multiple particle impacts.

The current model approximates the loading of polymer particles with copper nanoparticles simply as increase in the density of the particle. The interaction of the nanoparticles with the carries particle is a subject of future study. Also, how this phenomenon can be simulated to predict the polymer particle carrying nanoparticles impacting onto a substrate can be done by extending the current model.

REFERENCES

1. ARL, *Center for Cold Spray Cold Spray Process.* Retrieved 4 1, 2014, from http://www.arl.army.mil/www/default.cfm?page=370, 2010.

2. Wen-Ya Li, C.Z., Chang-Jiu Li, Hanlin Liao, *Modeling aspects of high velocity impact of particles in cold spraying by explicit finite element analysis.* Journal of Thermal Spray Technology, 2009. **18(5-6)**: p. 921-933.

3. Wen-Ya Li, W.G., *Some aspects of 3D numerical modeling of high velocity impact of particles in cold spraying by explicit finite emelent analysis.* Applied Surface Science, 2009. **255 (2009)**(2): p. 7878-7892.

4. H Assadi, F.G., T Stoltenhoff, H kreye, *Bonding mechanism in cold gas spraying.* Acta Meteriala, 2003. **51(2003)**: p. 4379.

5. Hussian, M., Shipway, Zhang, *Bonding mechanism in cold spraying: The contribution of metallurgical and mechanical components.* Journal of Thermal Spray Technology, 2009. **18 (3)**.

6. T Schmidt, F.G., H Assadi, H Kreye, Acta Meteriala, 2006. **54(2006)**: p. 729-742.
7. C J Li, W.Y.L., H L Liao, Journal of Thermal Spray Technology, 2006. **15(2006)**: p. 212-222.

8. K Yokoyama, M.W., S Kuroda, *Simulation of solid particle impact behavior for spray process.* Materials Transactions, 2006. **47(2006)**: p. 1697.

9. M Grujicic, C.L.Z., W S DeRosset, D Helfritch, Materiala Design, 2004. **24(2004)**: p. 681-688.

10. M Grujicic, J.R.S., D E Beasley, W S DeRosset, D Helfritch, Applied Surface Science, 2003. **219(2003)**: p. 211-227.

11. W Y Li, C.Z., X Guo, *Study on impact fusion at particle interfaces and its efect on coating microstructure in cold spraying.* Applied Surface Science, 2007. **254(2007)**: p. 517.

12. X L Zhou, X.Y.S., H Cui, *Effect of material properties of cold sprayed particles on its impacting behavior.* Acta Metallurgica Sinica, 2008. **44(2008)**(11): p. 1286.

13. Technology, S.D.S.o.M.a., *Cold Spray A guide to best practice.* 2012.

14. England, G., *Independent metallugist and consultant to the thermal spray coating industry.*

15. Baran Yildirim, S.M., Andrew Gouldstone, *Modeling of high velocity impact of spherical particles.* Wear, 2011. **270**(2011): p. 703-713.

16. King, B., Lee, *An experimental and finite study of cold spray copper impact onto two aluminum substrates.* Journal of Thermal Spray Technology, 2010.

17. Xiang-lin Zhou, X.-k.W., Hui-hua Guo, Jian-guo Wang, Ji-shan Zhang, *Depostion behavior of multi-particle impact in cold spraying process.* International Journal of Minerals, Metallurgy ad Materials, 2010. **17**(5): p. 635.

18. W Y Li, H.L.L., C J Li, G Li, C Coddet, X F Wang, Applied Surface Science, 2006. **253**: p. 2852-2862.

19. K Kang, S.Y., Y Ji, C Lee, Materials Science and Engineering, 2008. **486**: p. 300-307.

20. Johnson, C., *A constitutive modeland data for metals subjected to large strains high strain rates and high temperatures.* 1983.

21. Champagne, V.K., *The Cold Spray Materials Depostion Process: Fundamentals and Applications*. 2007, Cambridge: Woodhead Publishing.

22. Colak, O., *Modeling deformation behavior of polymers with viscoplasticity theory based on overstress.* Internation Journal of Plasticity, 2005. **21(2005)**: p. 145-160.

23. Ho, K., *Extension of the viscoplasticity theory based on overstress to capture non-standard rate dependence in solids.* Internation Journal of Plasticity, 2002. **18**: p. 851-871.

24. Krempl, H., *An overstress model for solid polymer deformation behavior applied to nylon 66.* ASTM STP, 2000. **1357**: p. 118-137.

25. Brockman, G.F.R., *A viscoelastic-viscoplastic constitutive model for glassy polymers.* Internation Journal of Solids and Structures, 2001. **38(2001)**: p. 5149-5164.

26. J Kim, A.M., *A time-integration method for the viscoelastic-viscoplastic analyses of polymers and finite element implementation.* Internation Journal for Numerical Methods in Engineering, 2009. **79**: p. 550-575.

27. Y. Xu, I.M.H., *Cold spray deposition of thermoplastic powder.* Surface and Coatings Technology, 2006. **201**: p. 3044-3050.

28. Kesavan Ravi, Y.I., Kazuhiro Ogawa, Tiana Deplancke, Oliver Lame, Jean-Yves Cavaille, *Mechanistic study and characterization of cold-sprayed ultra-high molecular weight polyethylene-nano-ceramic composite coating.* Journal of Thermal Spray Technology, 2015. **25**(1-2): p. 160-169.

29. Inc, J.S., *Material Properties Database, MPDB.*

30. Richeton, A., Vecchio, Jiang, Adharapurapu, *J.* Journal of Solids and Structures, 2006. **43**: p. 2318-2335.

31. Dean, M., *Determination of material properties and parameters required for the simulation of impact performance of plastics using finite element analysis.* 2004.

32. Laboratory, N.P., *Manual for the calculation of elastic plastic material model parameters.* 2007.

33. ABAQUS, *Academic Research User Manual Guide.* **In Release 6.14**.

34. McCrum, B., Bucknall, *Principles of ploymer engineering.* New York: Oxford University Press, 1997.

35. Israelachvili, J., *Intermolecular and Surface Forces*. 2nd Edition ed. 1991: Academic Press - An Elsevier Science Imprint.

36. Fowkes, F.M., Industrial and Chemical Engnieering, 1964. **56**(40).

37. Johnson, K.L., *Contact Mechanics.* Cambridge: Cambridge University Press, 1985.

38. Noppakun Sanpo, M.L.T., Phillip Cheang, K.A. Khor, *Antibacterial property of cold-sprayed HA-Ag/PEEQ coating.* Journal of Thermal Spray Technology, 2008. **18**(1): p. 10-15.

39. Bush, T.P., *Cold gas dynamic spray - characterization of polymeric deposition.* 2016.